

**CONTROL SYSTEM FOR PHASE-ONLY B_1 STEERING IN HIGH FIELD
MAGNETIC RESONANCE IMAGING**

A Thesis

by

KEVIN SHAILESH PATEL

Submitted to the Office of Graduate and Professional Studies of
Texas A&M University
in partial fulfillment of the requirements for the degree of

MASTER OF SCIENCE

Chair of Committee,	Steven M. Wright
Committee Members,	Mary P. McDougall
	Raffaella Righetti
	Laszlo B. Kish
Head of Department,	Miroslav M. Begovic

December 2019

Major Subject: Electrical Engineering

Copyright 2019 Kevin Shailesh Patel

ABSTRACT

In Magnetic Resonance Imaging (MRI) as the field strength is increased in order to achieve a higher signal to noise ratio (SNR), it becomes more difficult to image, requiring more advanced & expensive hardware, complicated pulse sequences, and different imaging techniques. 7 Tesla(T) MRI scanner are becoming more commonly used for clinical work and easier to access. The goal of this project was to build a control system capable of control a set of phase shifter dynamically in order to perform B_1 steering at 7T. B_1 steering refers to focusing the energy to a point in space to ensure a strong B_1 at that point. This is different than shimming, where the field is made more homogenous. However, in this thesis, the term B_1 shimming will be used as it is more common. The control system as well needs to perform diagnostics in order to guarantee correct operation.

B_1 shimming requires the ability to change phase for transmit power (TX) on each channel of a parallel transmit coil. While a simple approach to this problem would be to use a collection of coaxial cables of various lengths, this is very cumbersome and limits the functionality of the system. Therefore, a set of nonmagnetic digitally controllable phase shifters with 17 unique states were built in order to manipulate the phase on an 8-element dipole array coil designed by others in the lab. While the phase shifters and the coil, compose the front end of the system, an additional control system was still required.

Therefore, a third system was developed in order to control 16 phase shifters modules (8 low bit modules, and 8 high bit modules), measuring gain and phase on each

channel of the coil, and exercising the system in the lab, and to run diagnostics. The system will be developed so it can be tested & verify on the bench at the Magnetic Resonance System Lab (MRSL) at Texas A&M University(TAMU) in order to verify the results and experiments that were conducted at the University of Texas Southwestern medical center (UTSW) in Dallas, Texas.

The system was built using a microcontroller, evaluation boards, system onboard computer, and a host computer. The system can supply a DC load of up to 26A into the magnet room in order to power the entire system. The system is able to set the state of all the phase shifter in less than 10ms suitable for most multi-slice applications.

DEDICATION

To my family

ACKNOWLEDGMENTS

I would like to thank everyone that has supported me and have been involved with this project. First, I would like to thank my parents for their continued support for everything that I do. As well for teaching me from a young age the value of a good work ethic and how important it is to work hard in everything you do. My sister Manasi for always helping me show my parents that being a student often requires more hours than a full-time job. My aunt, and grandparents for always reminding of the important things in life.

My friends who were always willing and able to accommodate my very dynamic schedule and very random timings regardless of the affair or reason behind it. Their willingness to always listen to me vent and make bad jokes about the stress and heavy workload I was under and simply make my time in university more enjoyable.

My lab-mates who have guided me with their knowledge and skill have in order help me quickly adjust to the lab. Matthew Wilcox for rushing to the USB lab after a phone call or text messages of when something was not working perfectly, aid in finding bad SMA cables, and lastly for the building of the coil for this project. Chenhao Sun who started off as my mentor in the lab when I was only a summer student who with his “Make it work” catchphrase has spent countless hours with me in the lab past midnight to test the system. I as well acknowledge to everyone who worked on this project before I arrived in the lab, and unfortunately, I was never able to get acquainted with.

Dr. Steven Wright who has advised and guided me through this project. Who willing to accept my long list of questions on a weekly basis, responding to slack message within a few minutes any day between 8AM to Midnight (half of whom these questions made no sense due to lack of sleep), and lastly for always helping me simplify my very ambitious, outrageous, and just overly complicated approaches to very simple task. As well for building a lab specifically designed to help educate and train students like myself and others in not only theory but hands-on skills that can use distinguish ourselves and the skillset we hold as Electrical Engineers.

Unfortunately, I was not able to mention everyone that I would like, but their efforts are greatly appreciated.

CONTRIBUTORS AND FUNDING SOURCES

Contributors

This work was supervised by a thesis committee consisting of Professor(s) Steven M. Wright [advisor], Raffaella Righetti, and Laszlo B. Kish of the Department of Electrical and Computer Engineering and Professor Mary P. McDougall of the Department of Biomedical Engineering.

All work for the thesis was completed by the student, in collaboration with Chenhao Sun of the Department of Electrical and Computer Engineering and Matthew Wilcox of Biomedical Engineering. The student was also aided by Ivan Dimitrov and Sergey Cheshkov of the Advanced Imaging Research Center at the University of Texas Southwestern in collecting data and for time on the 7 Tesla MRI scanner.

Funding Sources

This work was made possible in part by the state of Texas under Grant Number RP160847 Its contents are solely the responsibility of the authors and do not necessarily represent the official views of the Cancer Prevention and Research Institute of Texas

NOMENCLATURE

AD8302	Analog Devices 8302 Evaluation Board
ADC	Analog to Digital Converter
BBB	BeagleBone Black
dBm	Power ratio expressed in (dB) referenced to 1 milliwatt (mW)
GPIO	General Purpose Input Output
MCU	Microcontroller Unit
MRI	Magnetic Resonance Imaging
MRS�	Magnetic Resonance Systems Lab
NF	Noise Floor
NMR	Nuclear Magnetic Resonance
PCB	Printed Circuit Board
RX	Receive Signal
SNR	Signal to Noise Ratio
T	Tesla
TPI	TPI Frequency Synthesizer
TX	Transmit Signal
UTSW	University of Texas Southwestern Medical Center
Preamp	Preamplifier
PA	Power Amplifier
VNA	Vector Network Analyzer

TABLE OF CONTENTS

	Page
ABSTRACT	ii
Dedication	iv
ACKNOWLEDGMENTS.....	v
CONTRIBUTORS AND FUNDING SOURCES.....	vii
NOMENCLATURE	viii
TABLE OF CONTENTS	ix
LIST OF FIGURES.....	xi
LIST OF TABLES	xiii
CHAPTER I INTRODUCTION	1
1.1 Difficulties of Imaging at 7 Tesla	1
1.2 B ₁ Shimming and B ₁ Steering	3
1.3 Thesis Organization.....	5
CHAPTER II BACKGROUND.....	7
2.1 Power Divider and Phase Shifter Background.....	7
2.2 Phantom and Dipole Coil	12
CHAPTER III SYSTEM ARCHITECTURE	14
3.1 Host Computer	16
3.3.1 GUI.....	16
3.2 Power Supply Unit	22
3.2.1 Current Requirements.....	22
3.2.2 BeagleBone Black (Bridge).....	23
3.2.3 RF Amplifiers Unit.....	24
3.3 Controller	26
3.3.1 Fiber Optic Communication.....	28
3.3.2 Controlling the Phase Shifters.....	29
3.3.3 Dynamically Controlling the Phase Shifters	30
3.3.4 In-Phase/Birdcage/Anti-birdcage Mode.....	34
3.3.5 Active Transmit/Receive Switches & Pin Diode Driver.....	34

CHAPTER IV REMOTELY MEASURING GAIN & PHASE	38
4.1 Using the AD8302 Evaluation Boards	38
4.2 Adapting the AD8302 For This System.....	44
4.3 Using the Measurement System.....	46
4.4 Noise Mitigation.....	47
4.5 Broadband Operation	51
CHAPTER V EXERCISING THE SYSTEM AS A WHOLE	54
5.1 Testing with the Positioner System.....	54
5.2 Testing on the 7T MRI System	62
CHAPTER VI CONCLUSIONS AND FURTHER DEVELOPMENT	65
6.1 Summary	65
6.2 Further Improvements	66
6.3 Conclusions	68
REFERENCES.....	70
APPENDIX A USER MANUAL AND DEBUG PROCEDURE	74
A.1 Launching the BeagleBone	74
A.2 Starting the Host Computer.....	77
A-2.1 Launching the Host Computer through Executables	77
A-2.2 Launching the Host Computer through Command line	78
A.3 Functions on the GUI	79
A.4 Setup Procedure for UTSW.....	80
A.5 Setup Procedure for MRSL	81
A.6 Debug Procedures.....	83
APPENDIX B PCBS.....	86
B.1 Motherboard	87
B.2 Power Supply Board.....	93
B.3 Pin Diode Driver.....	95
B.4 Trigger Interface for Dynamic Shimming	96
APPENDIX C MATLAB CODE FOR PROCESSING POSITIONER DATA	97
C.1 Function – pointsToSurf.m.....	97
C.2 Script – Positioner_Plot.m.....	98

LIST OF FIGURES

	Page
Figure 1.1 – Simulation of a B_1 Field at 7Tesla for Birdcage coil in a homogenous human body phantom	3
Figure 2.1 – Single stage 1 to 2 way Wilkinson power divider schematic	9
Figure 2.2 – Two stage 1 to 4 way Wilkinson power divider schematic	10
Figure 2.3 – Constructed two stage 1 to 4 way Wilkinson power divider	11
Figure 2.4 – Gelatin phantom with the 8 channel dipole array placed.....	13
Figure 3.1 – High level view of the communication layer of the control system	15
Figure 3.2 – Entire system that is placed throughout the MRI suite	16
Figure 3.3 – Static GUI window to be used for manual control operation	18
Figure 3.4 – Dynamic GUI window to be used for changing phase per slice select.....	19
Figure 3.5 – Terminate Test GUI window used to ensure the system is properly connected	20
Figure 3.6 –Phase shifter test GUI window if the phase shifters are functioning properly	21
Figure 3.7 – Power Supply Unit & BeagleBone(Bridge)/ RF Amplifier Unit.....	22
Figure 3.8 – Power Supply Unit and the housing of the BeagleBone(Bridge)	24
Figure 3.9 – RF Amplifier Unit used to generate high power RF signal for testing without the 7T scanner.....	26
Figure 3.10 – System Rack encasing the equipment placed in the magnet room	27
Figure 3.11 – Controller layout which houses the power supply board, measurement system, and microcontroller.....	28
Figure 3.12 – Timing of phase shifting being applied dynamically due to an external trigger.....	32
Figure 3.13 – Phase dynamically shifting after one trigger is applied.....	33

Figure 3.14 – Phase dynamically shifting after two triggers are applied.....	33
Figure 3.15 – Schematic for a 1 Channel pin diode driver using the designed topology	36
Figure 3.16 – The constructed 2 Channel Transmit/Receive pin diode driver.....	37
Figure 4.1 – Phase output of a single AD8302 evaluation board.....	40
Figure 4.2 – Hardware setup of the measurement system.....	41
Figure 4.3 – Phase output of using 2 evaluation boards with a hybrid coupler	42
Figure 4.4 – Phase output of the measurement system once the phase has been decoded	44
Figure 4.5 – Signal chain of the measurement system.....	45
Figure 4.6 – Accuracy of the measurement system compared to the VNA	47
Figure 4.7 – System connected for a signal channel using built shielded DE9 cables	48
Figure 4.8 – Process for finding the appropriate filter capacitor for the AD8302 evaluation board.....	50
Figure 4.9 – Measurement system components placed inside of the controller	52
Figure 5.1 – Positioner system being used with the liquid phantom.....	55
Figure 5.2 – Diagram of the positioner system setup with the developed body coil system	56
Figure 5.3 – Procedure for B ₁ Shimming using the positioner system at a fixed point ...	57
Figure 5.4 – Procedure for B ₁ Shimming by collecting eight B ₁ Maps	58
Figure A-1 – Power Supply Unit connected for operation	74
Figure A-2 – Terminal output of the BeagleBone being correctly launched	75
Figure A-3 – Terminal output of the Client Computer is correctly connected to the server	76
Figure A-4 – Desktop executable for the entire system	77
Figure A-5 – Terminal output of the client computer being correctly launched	78

LIST OF TABLES

	Page
Table 2.1 – S Matrix for the built 1-4 way High Power Wilkinson Power Divider.....	12
Table 3.1 – Current requirements of the system	23
Table 3.2 – Byte codes for the messages sent over the fiber optic Lines.....	29
Table 4.1 – Frequency bands of the components used in the measurement system	53
Table 5.1 – Simulations of B ₁ Shimming at 4 different focal points	60
Table 5.2 – B ₁ Shimming gain & phase field maps using the positioner system.....	61
Table 5.3 – B ₁ Shimming images using the 7T MRI system	64
Table A-1 – Functions on the GUI	80

CHAPTER I

INTRODUCTION

1.1 Difficulties of Imaging at 7 Tesla

In Magnetic Resonance Imaging (MRI), The first step in any scan is using an RF pulse to “excite” spins, to create a signal [1]. This requires a very uniform RF field both in amplitude and phase. Unfortunately, as the frequency of research scanners increase the difficulty in imaging does as well. While the general idea of imaging at higher field strengths does not change from imaging at lower fields, it requires more advanced hardware, pulse sequences, and imaging tactics.

In MRI, the pursuit of acquiring higher contrast [2] [3], higher resolution, and higher Signal to Noise ratio (SNR) has been the driving point of moving to higher magnetic field strength [4]. The desire of moving to higher magnetic field strengths has been around since the early days of MRI and more recently the field is moving towards at 7 Tesla(T) for clinical work and research.

Imaging at 7T has presented many issues due to the requirement of having to use high frequency. Directly related to the Larmor frequency of water imaging at 7T requires a frequency of 298MHz. The most dramatic issues have come to be an increase in the Specific Absorption Rate (SAR), non-uniform B₁ field, higher sensitivity to artifacts, and a higher economic cost [5].

$$f = \frac{\gamma B_0}{2\pi} \tag{1.1}$$

$$\gamma = 2\pi * 42.57 \frac{MHz*rad}{T}, B_0 = 7T \tag{1.2}$$

$$f = \frac{1}{2\pi} * (2\pi * 42.57 \frac{MHz}{T}) * 7T = 298 MHz \quad (1.3)$$

Traditionally the birdcage coil has been used for decades in MRI for large volume imaging at clinically at lower field strengths such as 1T or 3T. A birdcage coil requires that phase shifter is equally distributed over 6 or more channels. An equally distributed phase shift is applied between each element to get a full range phase shift.

$$\Delta\phi(\text{degrees}) = \frac{360^\circ}{N} \quad (1.4)$$

The birdcage coil is not an option 7T due to generating a large variation in B_1 at in throughout the volume of the phantom. Furthermore, the artifacts are produced such as “central brightening” [4] [5] [6]. Figure 1.1 is a simulation of an 8 element birdcage coil on a body phantom it can be seen that throughout there is not a region of sufficient B_1 . Even though the phantom itself is homogenous, but the B_1 field is changing very sporadically. Imaging with insufficient B_1 essentially means that not enough signal was received to obtain any spatial information from that location. This is dealt with by performing B_1 shimming or steering the beam to various points of interest (or focal points) on the phantom.

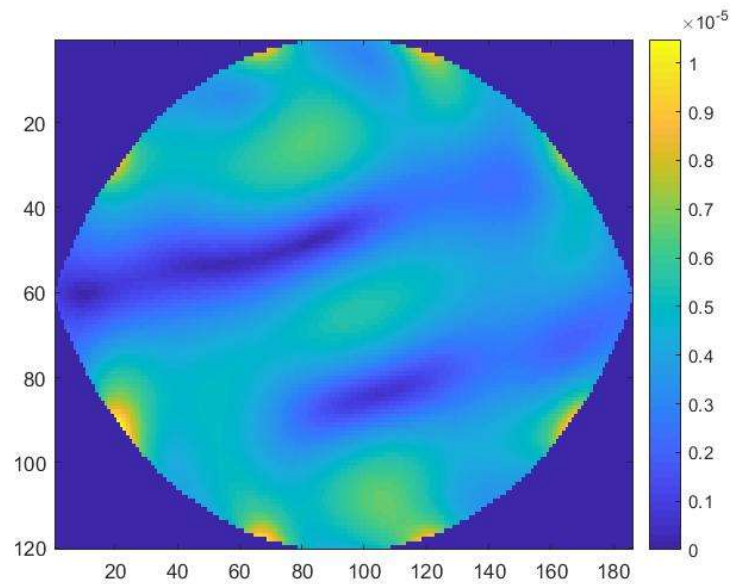


Figure 1.1 – Simulation of a B_1 Field at 7Tesla for Birdcage coil in a homogenous human body phantom

1.2 B_1 Shimming and B_1 Steering

Traditionally in Magnetic Resonance Imaging one factor of controlling the image quality has been through the process of shimming. Shimming is the act of increasing the homogeneity of the magnetic field in order to reduce magnetic susceptibility that is introduced when using different phantoms, but has typically been done on the static magnetic field (B_0 field) [7]. B_0 Shimming is the process of changing the DC current on the various axis of the magnet itself in order to get a precise and continuous magnetic field and remove areas of local susceptibility. While this has been typically been the standard since the beginning days of MRI, but this is not as sufficient for high field MRI (7T or higher).

B_1 shimming (or RF shimming) on the other hand is the process of using the Transmit power to directly shim upon the induced magnetic field(B_1 field) [8]. Doing so gives the ability to disregard the local inhomogeneity from the B_0 field and characterize the phantom based solely on the B_1 field [8]. B_1 Shimming relies on the ability to manipulate the induced current on the phantom this is done changing the amplitude and phase on transmit signal on a multi-channel system to construct or destruct the B_1 field [9]. B_1 shimming is therefore capable of forcing the induced magnetic field to be more homogenous and uniform [10].

B_1 steering(or beam steering) on the other hand is focusing energy at a point of interest to achieve plenty of B_1 . This allows the B_1 to be concentrated in certain regions, counteracting the issue with the birdcage coil to appear bright at the center and is capable of generating an acceptable amount of B_1 at a specific point. B_1 steering does require precise control over the amplitude and phase of the transmit signal over multiple channels.

In order to B_1 shim or B_1 steer, prior knowledge of the B_1 field is necessary, this requires that the induced magnetic field is mapped (B_1 mapping) this is performed which is the process of acquiring images that relate that phantom to the RF parameters amplitude and phase for each voxel. Once the B_1 maps are acquired they are read into an algorithm in order to generate phase solutions(or shim solutions). for the imaging area of interest. Phase solutions are simply a set of phase shifts applied for each channel of the transmit signal.

Normally B_1 Steering has been performed using control over both amplitude and phase, but it is possible to do so using only phase control with sufficient resolution. B_1

Steering requires SAR monitoring in order to avoid heating of the phantom. Ideally, the easiest way to prevent issues with SAR is to not use control over amplitude [11]. Furthermore, controlling amplitude is quite difficult as not very impactful as phase control [12]. It has been demonstrated by Gregor Adriany [6] and PF Van de Moortele [13] that phase control is more significant than amplitude control for B_1 shimming. B_1 Shimming can be performed using only phase control, but this requires sufficient control over multiple transmit channels.

Typically, B_1 steering has been performed statically which results in a small circular region that can be focused throughout the phantom by changing phase solutions per imaging. In order to increase the size of the focused region requires the ability to perform B_1 steering dynamically. This means that a unique phase solution is used for each slice selected throughout the imaging process.

For this thesis, the terms B_1 shimming and shim solutions, as opposed to B_1 steering and phase solutions, will be used as it is more common in literature.

1.3 Thesis Organization

This thesis describes the control system designed and built in order to control a set of 16 digitally controlled phase shifters for B_1 shimming at 7T for a Human Body Phantom using an eight-channel array. This system aims to dynamically control these phase shifters in less than 10ms and as well used feedback in order to monitor the status of the system for diagnostics. The system was tested in the lab using a positioner system to collect field

maps in order to understand the operation of the system. It was then tested on the 7T MRI scanner at the University of Texas Southwestern.

An overview of 7T imaging is given along the idea of B_1 shimming in Chapter I. Chapter II then goes into the background of the project and description of the work done by colleagues which are vital parts of this system. Chapter III goes into the system architecture and an explanation of how the different aspects of the control system interact and communicate within itself. The system will need to be assembled in a modular fashion for easy transportation from MRS� to UTSW, and nonmagnetic for use near the magnet bore. Additional clarification is given on how the system can be easily operated by the user. Chapter IV goes into an explanation of the measurement system and the design of how to reduce the complexity of setup. The measurement system was required to be accurate within 22.5° of phase resolution. Afterward, in Chapter V the testing of the system and results collected in the lab at the Magnetic Resonance System Lab at Texas A&M University and the 7 Tesla MRI scanner at the University of Texas Southwestern. Finally, Chapter VI gives an overview of this thesis, a brief conclusion on the work done and as well mentions the potential for improvements.

CHAPTER II

BACKGROUND

2.1 Power Divider and Phase Shifter Background

Shifting the phase of the RF signal can be shifted multiple ways the most common ways to do this to use transmission lines of variable length [6] [13] [14] [15]. Using transmission lines, the phase of the RF signal can easily be increased or decreased by changing the length of RF cables(transmission line). Cables lengths can be calculated by easily taking the velocity of the signal through transmission line which is simply the speed of light multiplied by the velocity factor of the cable divided by the frequency of the signal to get the wavelength. The phase is then just the ratio between the length of the cable and wavelength multiplied by 360° or 2π in order to convert from percent of wavelength to degrees or radians respectively.

$$v_f C = \lambda f \quad (2.1)$$

$$\frac{v_f C}{f} = \lambda \quad (2.2)$$

$$\phi(\text{degrees}) = \frac{L}{\lambda} * 360^\circ \quad (2.3)$$

$$\phi(\text{radians}) = \frac{L}{\lambda} * 2\pi \quad (2.4)$$

Simply changing RF cables of variable length on the transmit path is sufficient for B_1 shimming at a given point. The issue with this is method is that it is quite cumbersome as it requires an individual to manually change the cable. Having an individual manual changing the cables do not allow the ability to shim dynamically per slice select [15].

Another approach to B_1 shimming would be to use multiple RF power amplifiers, each operating independently [7] [16]. This would that in order to shift the phase it only requires the input phase to be varied on each amplifier using I/Q modulation. While this approach does allow the ability to dynamically B_1 shim it can be very expensive and difficult to obtain multiple power amplifiers [16].

Therefore, a set of digitally controllable Phase shifters were designed and built by others in the lab. Research conducted in the lab has found in order to adequately perform B_1 shimming a minimum phase resolution of 45° is required. This phase shifters are designed to allow a full range phase shifting with a step size of 22.5° along with a 50Ω termination. These phase shifters work by using a combination of transmission lines and lumped elements to shift the phase of a 298MHz RF signal or even terminate the signal to 50Ω . In order to control the phase, shifter, it requires 5 bits of control per channel and a total of 17 unique states. Essentially any phase shift can be constructed by using a combination of the $22.5^\circ, 45^\circ, 90^\circ$, and 180° phase shifts. Switching between states has been found to be less 3ms for the phase alone sufficient for B_1 Shimming.

One of the major disadvantages of the phase shifters is the large power required to properly operate the device. Each phase shifter module requires 600mA at 5V and 20mA at -48V. The system as a whole uses 16 phase shifter modules resulting in 9.6A at 5V and 320mA at -48V. This generally would be considered a very large current draw in MRI. Due to close proximity to the magnet, a current carrying wire could behave a shim and possibly distort the B_0 field.

In order to get multiple, transmit signals and avoid the additional cost of buying power amplifiers which can be very expensive. Two four-way Wilkinson Power Dividers were built in order to utilize both power amplifiers available at the University of Texas Southwestern. Doing so eight phases identical transmit signals are available with equal amplitude and phase.

The power divider(or power splitter) could be constructed in 2 manners that result in a 1 to the 4 way splitter. The first method is a single stage 1 to 4 way splitter, and the second method requires building 2 stages of 1 to 2 way splitter cascaded with another 1 to 2 way splitter on both ends to get 4 outputs. Figure 2.1 shows a single stage 1 to 2 way splitter. Due to the product of the characteristic impedance and square root of the number of ports being directly related to the characteristic impedance of the transmission line needed both types of power dividers will require different transmission lines [17]. The equations below show that a 2 way splitter requires 70.71Ω and 100Ω for a 4-way splitter.

$$Z_{TL} = \sqrt{N} * Z_0 \quad (2.5)$$

$$2 \text{ way spilter: } Z_{TL} = \sqrt{2} * 50 = 70.71\Omega \quad (2.6)$$

$$4 \text{ way spsilter: } Z_{TL} = \sqrt{4} * 50 = 100\Omega \quad (2.7)$$

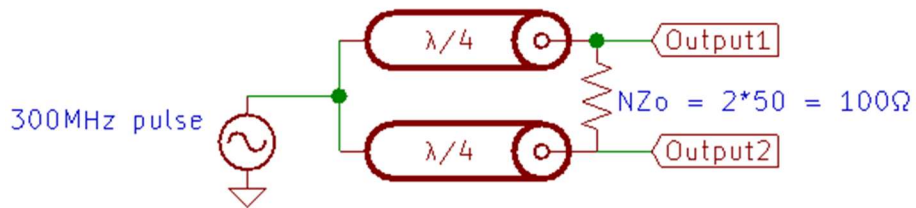


Figure 2.1 – Single stage 1 to 2 way Wilkinson power divider schematic

Ultimately it was found that the 100 Ω coaxial cable is very difficult to obtain in small batches, but 73Ω can be purchased easily. The difficulty in acquiring 100Ω coaxial lead to the decision to build a 2 stage of 1-2 way splitter cascaded as 73Ω can be acquired easily and is very close to the required value. Figure 2.2 shows the two stages of the 1 to 2 way Wilkinson power divider cascaded. Figure 2.3 shows the constructed power divider using two stages of the 1 to 2 way Wilkinson power divider cascaded.

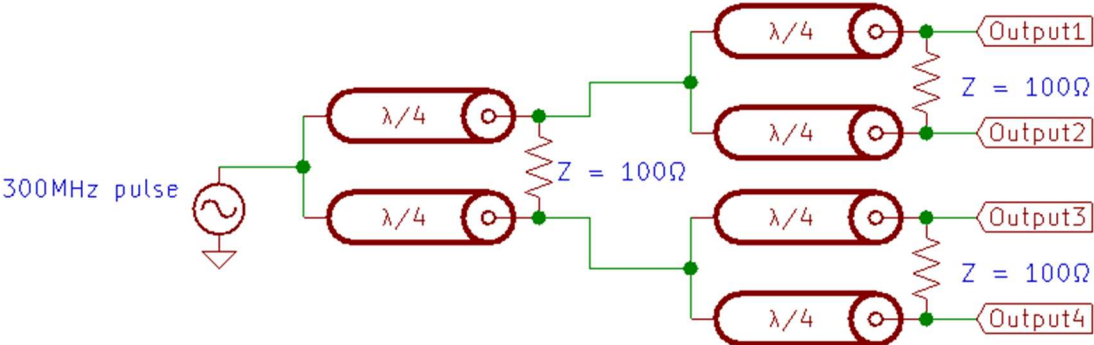


Figure 2.2 – Two stage 1 to 4 way Wilkinson power divider schematic

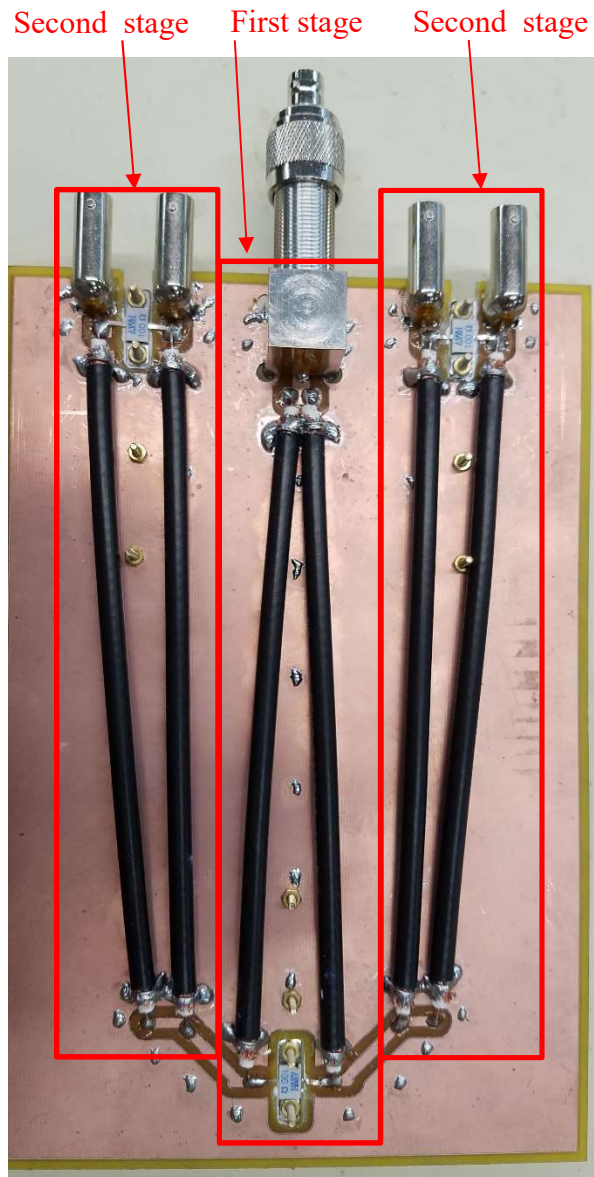


Figure 2.3 – Constructed two stage 1 to 4 way Wilkinson power divider

The S-matrix in Table 2.1 shows when using port 1 as the end up the power outputted on the other 4 ports is roughly 6.3dB. As 6db is required for a 4 way splitter the excess loss is only .3 dB. The phase as well is found to be only about 1° . The low excess

loss and very low phase imbalance show that 4-way divider is correctly operating for applications requiring 50Ω characteristic impedance.

S-Matrix Rx	Tx	1	2	3	4	5
1		-12.5 dB	-6.30 dB 71.8°	-6.36 dB 72.9°	-6.39 dB 71.4°	-6.30 dB 70.2°
2		-6.27 dB 72.3°	-17.6 dB	-38.9 dB 78.4°	-26.7 dB 131.7°	-27.8 dB 120.6°
3		-6.33 dB 73.5°	-36.0 dB 74.0°	-19.3 dB	-27.9 dB 130.0°	-28.0 dB 120.9°
4		-6.36 dB 72.1°	-27.1 dB 127.8°	-28.2 dB 130.0°	-19.7 dB	-35.9 dB 34.5°
5		-6.27 dB 71.4°	-26.7 dB 130.0°	-27.7 dB 128.1°	-35.9 dB 38.8°	-17.6 dB

Table 2.1 – S Matrix for the built 1-4 way High Power Wilkinson Power Divider

2.2 Phantom and Dipole Coil

Two human body size phantoms were built by others in the lab along with an 8 element Dipole array Coil. The Dipole coil was constructed using on 1oz copper-clad FR4 board and milled on the LPKF. Each individual dipole element is 37cm in length with a width of 1cm and 1/8” base for separation from the phantom. The dipoles are each fed at the center using a match/tune board, and a balun to eliminate cable currents. Additionally, each channel contains a shielded current loop with a diameter of 7mm, aligned perpendicular to the B_1^+ field to receive maximum signal for the measurement system. Floating cable traps were used on the probes in order to mitigate cable interactions.

Both phantoms were constructed out of PVC pipes, cut and sanded to be an almond shape and of identical size to represent the average human body [18] with inner dimensions of 35.5 cm by 26 cm, depth of 40cm, and an aperture angle of 147°. The phantoms were constructed to have a conductivity of 0.32 S/m and a dielectric constant of 45 [19]. The phantoms used a 4:1 volume ratio of corn syrup to distilled water with salt to achieve the correct conductivity. The major difference is that one phantom was gelatinized using Agarose for testing in the 7T MRI scanner at the University of Texas Southwestern to avoid motion artifacts. The second phantom of the same material but without the gelatin to be used in the lab for testing in the lab with the positioner system. Figure 2.4 shows a gelatin phantom that was used for testing in the 7T MRI scanner at the University of Texas Southwestern.

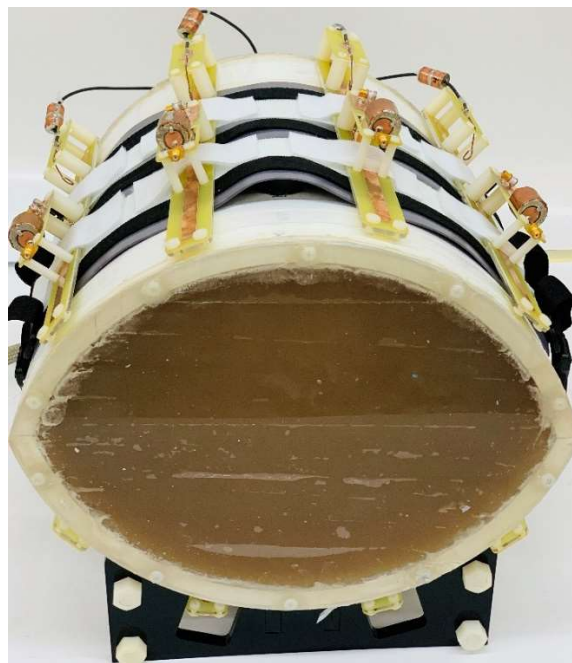


Figure 2.4 – Gelatin phantom with the 8 channel dipole array placed

CHAPTER III

SYSTEM ARCHITECTURE

In order to properly use this system, it had to be designed to operate within the 7T scanner at UTSW and independently in the lab at MRSL. The system had to be designed in a modular fashion so that can be taken apart and put together very easily. The system as well needed to operate accurately in both environments regardless of any noise that may occur from the 7T system or the lab equipment. In order to easily adapt the system to the host scanner the system needed to operate near the B_0 field, but this requires that the system is designed to be nonmagnetic. Due to the power supplies not being available inside the magnet room the system has to be able to move a large amount of current into the magnet room. Most importantly the system has to be designed so that it operates independently of the 7T scanner and does not have any cross-talk between the high frequency noise from the gradients or the rf amplifiers.

The system is designed so that control equipment is placed in 3 various locations around the MRI suite. The system operates by using a host computer in the control room for this a Microsoft Surface was used, in the server room is a BeagleBone Black (BBB), and lastly in the magnet room is microcontroller (MCU) in which an Atmel128 was chosen. The system is designed to work in master (Host computer) – bridge (BeagleBone Black) – slave (Atmel 128) architecture. The Host computer is the only device that can act on its own or takes inputs from the user, while the rest of the devices idle and wait for a task. The BeagleBone black is configured to be an interface for the rest of the control

objects. The Atmel128 is responsible for controlling the phase shifter and making measurements from the coil. Figure 3.1 shows a high level overview of the communication layer. The entire system that is shown for testing in the 7T MRI scanner is shown in Figure 3.2.

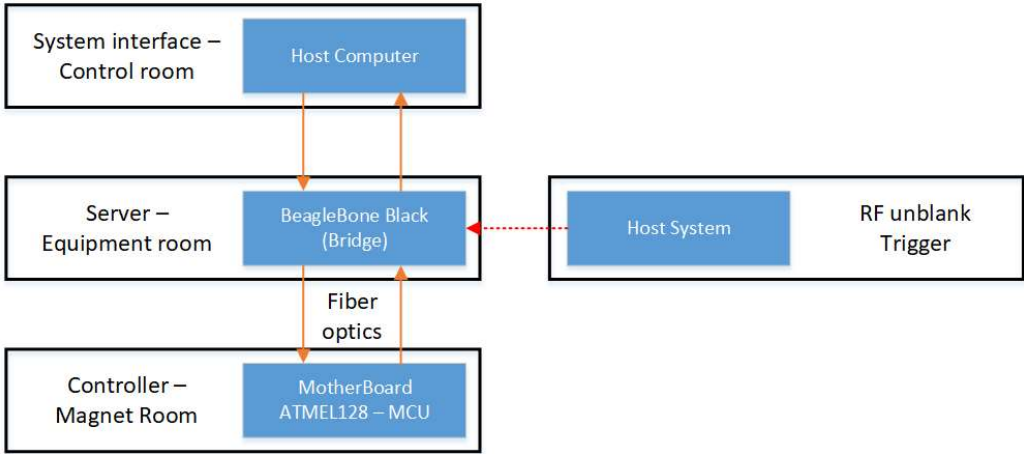


Figure 3.1 – High level view of the communication layer of the control system



Figure 3.2 – Entire system that is placed throughout the MRI suite

3.1 Host Computer

3.3.1 GUI

The Graphical User Interface (GUI) for the control system was designed to be very easy to operate. Using the python module PyQT5 the GUI was designed to control the entire system and be completely click/tap based for simple operation. Three different sets of windows for use in static operation, dynamic operation, and a test window.

The static window allows the complete control of operating the entire system. This includes setting the phase shifter, using the measurement system, control of the TPI, and

the state of the clock on the microcontroller. This window is designed is more useful for the development and validation of the system.

The static window allows the user to set the phase shift on each individual channel. The response can then be measured using the measurement system where the recorded measurements are then placed under the column measured phase. Typically, the measurement system is placed in normalize phase mode which will reference channel 1 for all of its measurements. The issue is that normalize does not easily represent the phase shifting on channel 1 as it will be referenced to zero while the other 7 channels will see an identical phase shift. Figure 3.3 shows static operation GUI without placing the system in the normalized mode so that the phase shift on channel 1 can be seen.

The GUI as well allows an individual to request any phase shift that is desired even if it not in the resolution of the phase shifter. The system will then first find a phase shift that is congruent and then find the closest phase shift that is possible to achieve using the phase shifters. The user will type in the requested phase shift in the Desired phase shift column and the actual phase shift achieved will be placed in the set phase column.



Figure 3.3 – Static GUI window to be used for manual control operation

The dynamic control window was designed with limited user input is shown in Figure 3.4. This operation will automatically shut off the TPI and control the state of the MCU’s clock. This window requires that the user to type in a table for every shim solution per RF pulse or simply read in a prewritten CSV table with the data already saved. The control system is then able to the state of all the phase shifters and will use the RF amplifier’s trigger from the scanner. Lastly, any under desired user input will shut down the control in order to protect the phase shifter from being damaged.

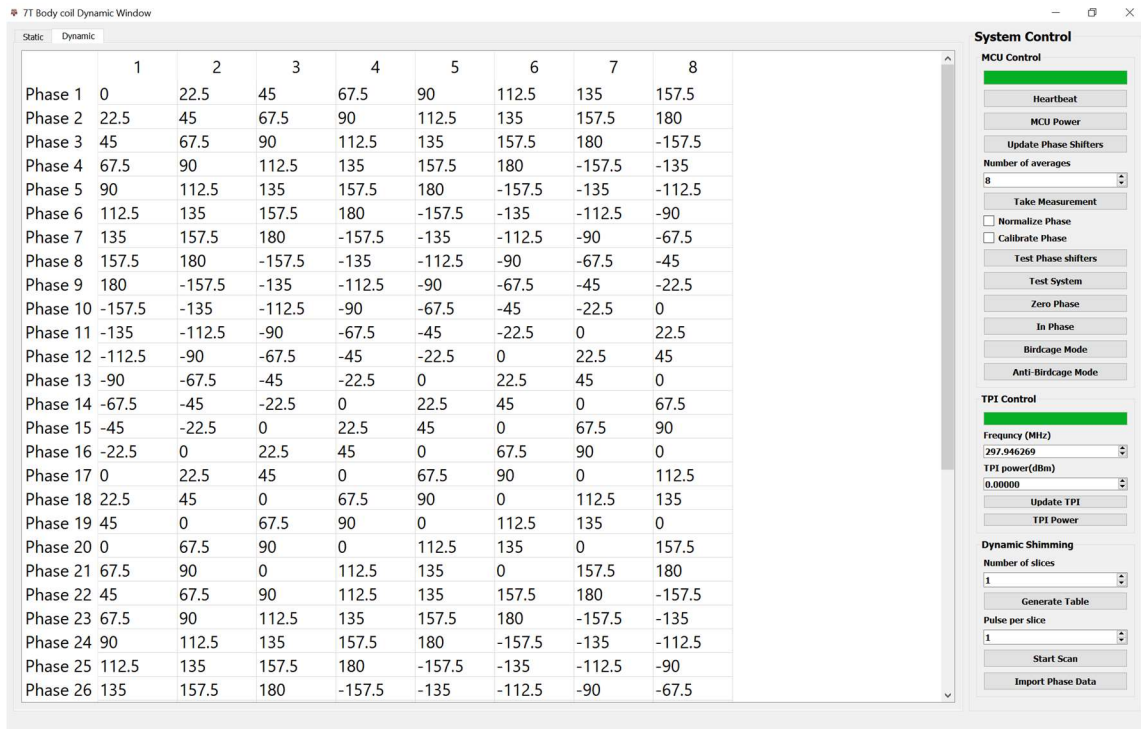


Figure 3.4 – Dynamic GUI window to be used for changing phase per slice select

Additionally, the third window with no user input was designed for quick system-validation of the entire system. This window runs two different tests the first test is designed to make sure that the system has been correctly connected and set up the system as a whole. This test is performed by simply terminating a single channel at a time and then using the measurement system to measure the gain and phase on all eight channels. While running this test the system would expect that only that was not terminated would see an effect and the other seven channels would not notice any significant changes for gain and phase.

Ideally, the user would expect a red diagonal line for the gain and another for phase. Figure 3.5 shows that since the window has a red diagonal on the top half of the

table so therefore there is not an issue with gain measurements. While the phase did not get a red window, this means there is a natural phase offset in the system due to dipole placement, the nonlinearity of the phase shifter, cable length, etc. , but this is not a major issue as it can be corrected by changing the default state of the phase shifter to compensate for the error.

The screenshot shows a 'Dialog' window titled 'Terminate Test' with a 'Phase shifter test' tab. The table below contains the data displayed in the window. The columns represent Coils 1 through 8, and the rows represent Gain and Phase measurements for Terminate states 1 through 8, plus a 'None' state. The 'Gain, Terminate 7' row is highlighted in blue, and several other cells are highlighted in red or green.

	Coil 1	Coil 2	Coil 3	Coil 4	Coil 5	Coil 6	Coil 7	Coil 8
Gain, Terminate None	11.279	12.254	9.857	11.51	11.356	12.627	7.632	8.04
Gain, Terminate 1	1.329	12.699	10.522	11.205	11.507	12.034	7.206	8.538
Gain, Terminate 2	12.039	0.124	10.969	11.976	11.698	12.659	8.204	7.966
Gain, Terminate 3	11.425	11.904	-1.695	12.969	11.692	12.566	7.113	8.146
Gain, Terminate 4	10.821	13.136	13.053	2.46	11.446	12.476	8.22	8.983
Gain, Terminate 5	11.557	12.934	11.131	11.475	1.777	13.731	8.12	8.424
Gain, Terminate 6	11.255	12.251	11.096	10.924	12.246	-0.289	9.653	8.814
Gain, Terminate 7	11.356	12.696	10.702	11.369	11.189	13.223	4.309	10.087
Gain, Terminate 8	11.7	12.293	11.441	11.867	11.017	12.884	10.432	3.49
Phase, Terminate None	0.0	-2.67	3.06	7.79	10.43	6.01	-15.47	24.64
Phase, Terminate 1	125.79	-4.11	10.13	9.78	11.49	2.8	-13.18	20.71
Phase, Terminate 2	-6.4	-176.42	-3.7	12.85	9.54	9.24	-12.12	27.83
Phase, Terminate 3	1.3	-11.04	-125.43	4.51	11.55	9.35	-13.19	25.05
Phase, Terminate 4	-3.19	7.67	5.24	-168.18	6.5	6.05	-17.65	20.17
Phase, Terminate 5	0.21	1.06	8.85	4.89	144.42	-5.29	-18.2	27.6
Phase, Terminate 6	-3.13	0.35	11.46	9.49	0.8	145.71	-19.36	26.31
Phase, Terminate 7	1.25	0.07	9.78	7.34	8.04	2.57	-179.18	11.75
Phase, Terminate 8	-0.99	0.29	5.97	8.54	10.96	8.79	-10.46	-173.95

Figure 3.5 – Terminate Test GUI window used to ensure the system is properly connected

The second test is the validation of all the phase shifters this is done by switching through all the different states on phase shifters for each channel. A single channel is tested one at a time, but every channel is measured during the test. Assuming the phase shifter does not have any error, the channel under test should see a linear phase shift with

a resolution of 22.5° and channel only see minor phase shift due to electromagnetic coupling. The result of the phase shifter test is eight graphs where each channel has 8 traces each, but only one trace has a linearly increasing phase shift.

Figure 3.6 shows that since all eight graphs are moving linearly upwards for every single point the phase shifter are working as expected. It can also be seen that changing that phase on one channel does cause the phase on another channel to change as well due to the coupling between the coil elements, but luckily it is not very large and significant to prevent being able to change the phase on another channel.

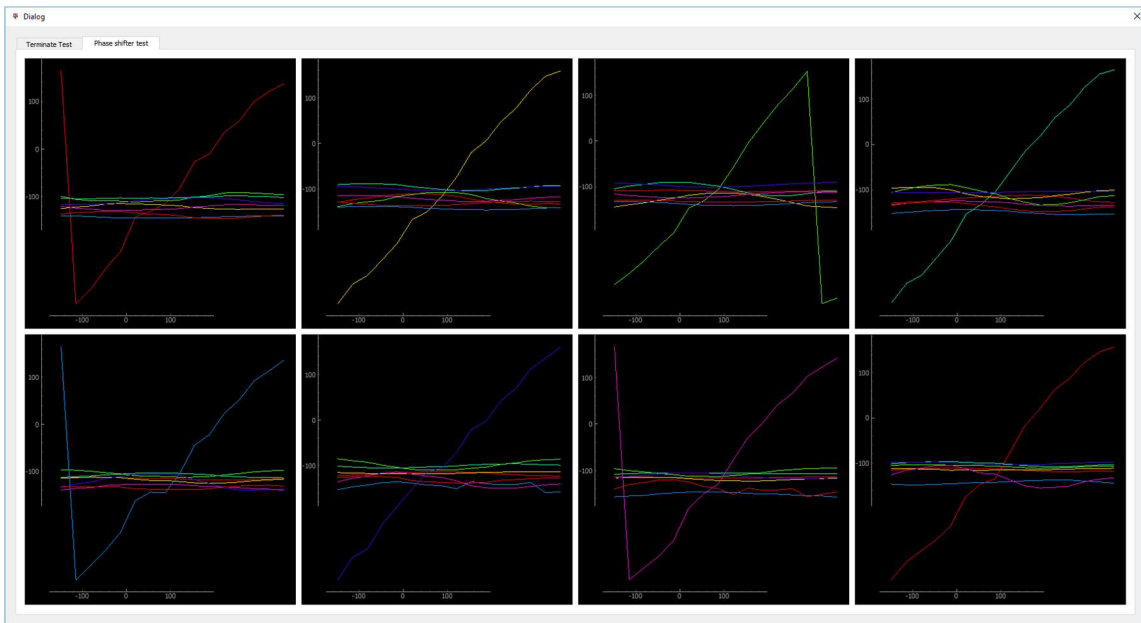


Figure 3.6 –Phase shifter test GUI window if the phase shifters are functioning properly

3.2 Power Supply Unit

The equipment placed in the server is composed of three small instruments responsible for supplying all of various power levels for equipment inside of the magnet room, housing of a BeagleBone Black to behave as a bridge between the equipment in the magnet room and the host computer, and last a set of RF amps for when the 7T system is not accessible or required is shown in Figure 3.7.



Figure 3.7 – Power Supply Unit & BeagleBone(Bridge)/ RF Amplifier Unit

3.2.1 Current Requirements

The power supply unit is placed in the server room and is responsible for supplying the DC power for the entire system. The system was configured to use 4 different voltages 5V, 7.5V, 15V, and -48V. Within the magnet room, high current is necessary therefore

two different 7.5V power supplies, 15V and -48V power is brought in over a 12/5 cable. The table below shows that most of the current is necessary for 7.5V supply which is crucial as it will get regulated down to 5V for powering of the phase shifters. The power supply unit is power by connecting an AC power cord from the wall outlet to the back of the unit. The Current requirements are further shown in Table 3.1

Voltage (V)	Current (A)	Purpose
5	1	Powering of the BeagleBone Black
7.5	12.8	Regulated done to 5V to power phase shifters and control equipment(MCU, AD8302, Switching matrix, etc..)
15	1.2	Power the 3.2W power amplifiers Regulated down to 12V to power the preamp in the measurement system
-48	1	Reverse bias supply for phase shifters and T/R switches

Table 3.1 – Current requirements of the system

3.2.2 BeagleBone Black (Bridge)

In order to allow an easy setup a single set up the Host Computer connects to the BeagleBone over a single RJ-45 connection, and then BeagleBone Black interfaces with the MCU through UART messages in the fiber optic lines, the TPI frequency synthesizer which communicates over UART messages over a mini USB and a reads trigger from the scanner on when to change states of the phase shifters. The BeagleBone Black is able to interface with the host computer using the python module PyZMQ. This allows the host computer to write an asynchronous message over an open port over to the BeagleBone access through the IP address. The BeagleBone is configured to simply just wait for

incoming messages from the Host computer for which it will then relay the message to its destination. Figure 3.8 shows the layout of these components inside of an enclosed aluminum case.

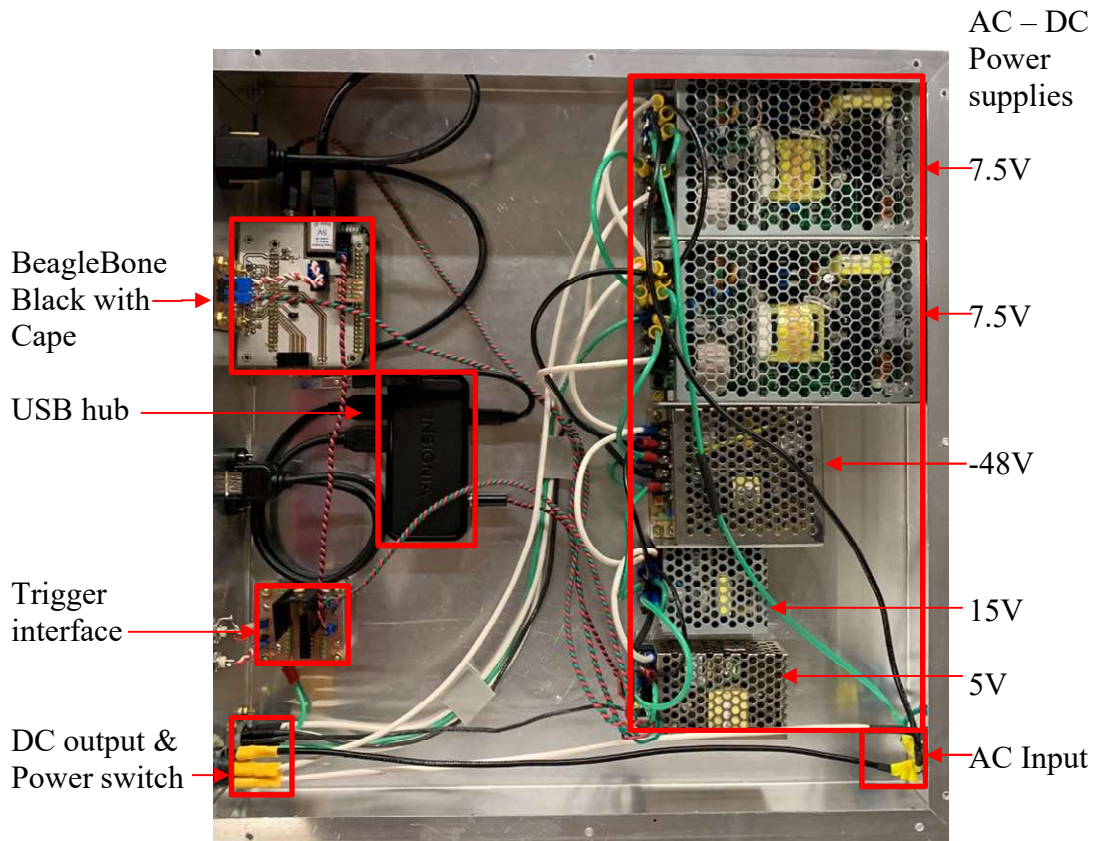


Figure 3.8 – Power Supply Unit and the housing of the BeagleBone(Bridge)

3.2.3 RF Amplifiers Unit

In order to allow this system to make meaningful measurements regardless of whether it was operated at the lab or UTSW, it was designed specially to work independently of the MRI Scanner. Two 3.2W RF PA (Power Amplifiers) were used to generate a continuous 298MHz signal that takes an input signal solely from the TPI. The

TPI is used in conjunction with a 4x1 RF power splitter in order to generate 2 signals where 2 are used to power the 3.2W RF PAs, the third output is used as the reference signal for AD8302 evaluation boards(AD8302), last output is then terminated to 50Ω. This RF amplifier was specifically chosen due to the high gain of 30dB and output power of 3.2W. While the system contains significant loss through the transmit chain 2 PA of 3.2W each was enough to make accurate measurements using the measurement system and the positioner.

Due to the PAs not being in encased and having poor shielding the items were placed in a large box to be spaced out to properly prevent cross talk. Furthermore, placing the amplifiers in a large box leaves room for more equipment for future development. This unit could easily be retrofitted for operation where a high power RF signal is needed within the frequency range of 1MHz to 700MHz.

The RF amplifiers require 15V and 700mA of current for both amplifiers. In order to bring power into the rf amplifier unit, two banana plugs were placed on the outside of the case. Banana plugs were originally chosen so that the unit could be used by using a bench power supply(which already has banana plug for its output) for when the entire developed system is not required , or the unit can pull power from the 15V supply on the power supply unit which has also been placed with banana plugs for its output. All of the components aligned inside of an aluminum case is shown in Figure 3.9.

It was later deemed that the banana plugs were not a good fit as it can easily be shorted if the power line(plugged into the red port) and the ground line(plugged into the black port) could be mixed and shorted if not properly connected. In the future, the banana

plugs would be replaced with another connector that is more user-friendly and cannot be shorted so easily.

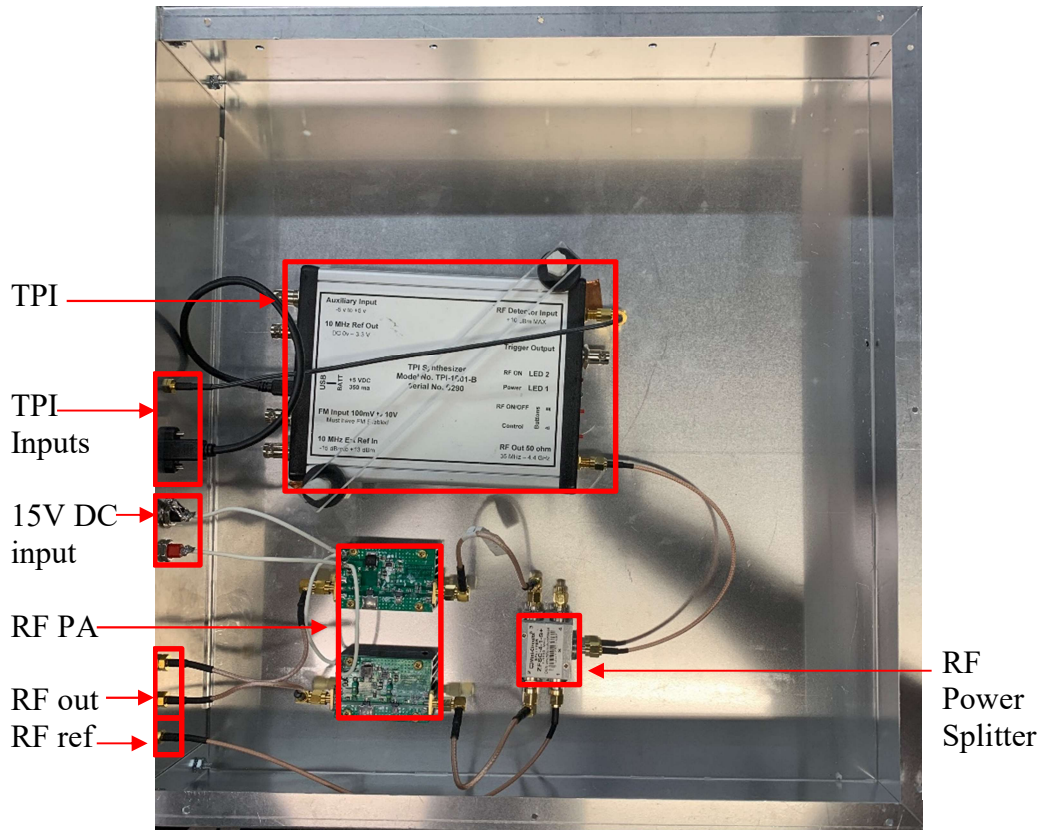


Figure 3.9 – RF Amplifier Unit used to generate high power RF signal for testing without the 7T scanner

3.3 Controller

The controller houses the microcontroller and designed to be non-magnetic as it is placed near the magnet room is the bottom of the system rack, encompasses three smaller

subsystems one for setting states on all the phase shifters, the measurement system for calculating gain and phase, and a lastly active T/R switches and a pin diode driver. The entire controller is driven by the Atmel128 microcontroller. Similar to the BeagleBone the MCU will wait for commands and act upon it and then go back to idling. An additional requirement of the MCU is that it is required to have its clock shut down in order to avoid artifacts during imaging. Figure 3.10 shows the units designed inside of the system rack. While Figure 3.11 shows a more in depth look at the measurement system.

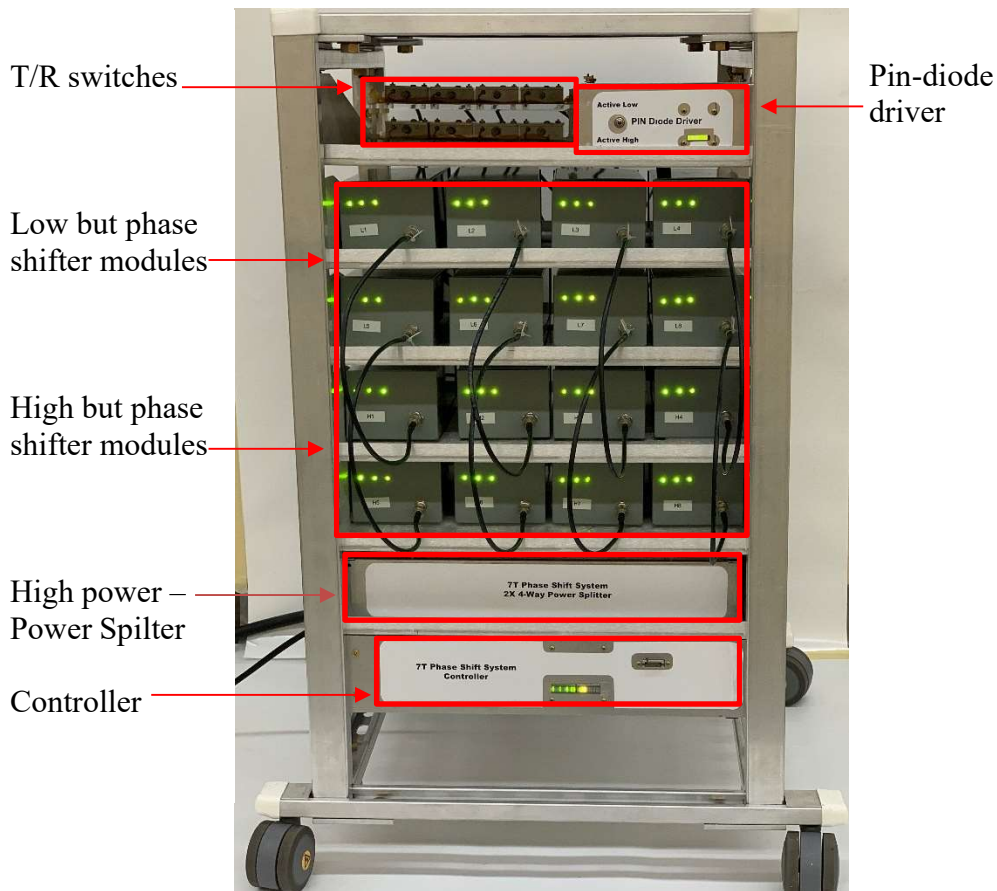


Figure 3.10 – System Rack encasing the equipment placed in the magnet room

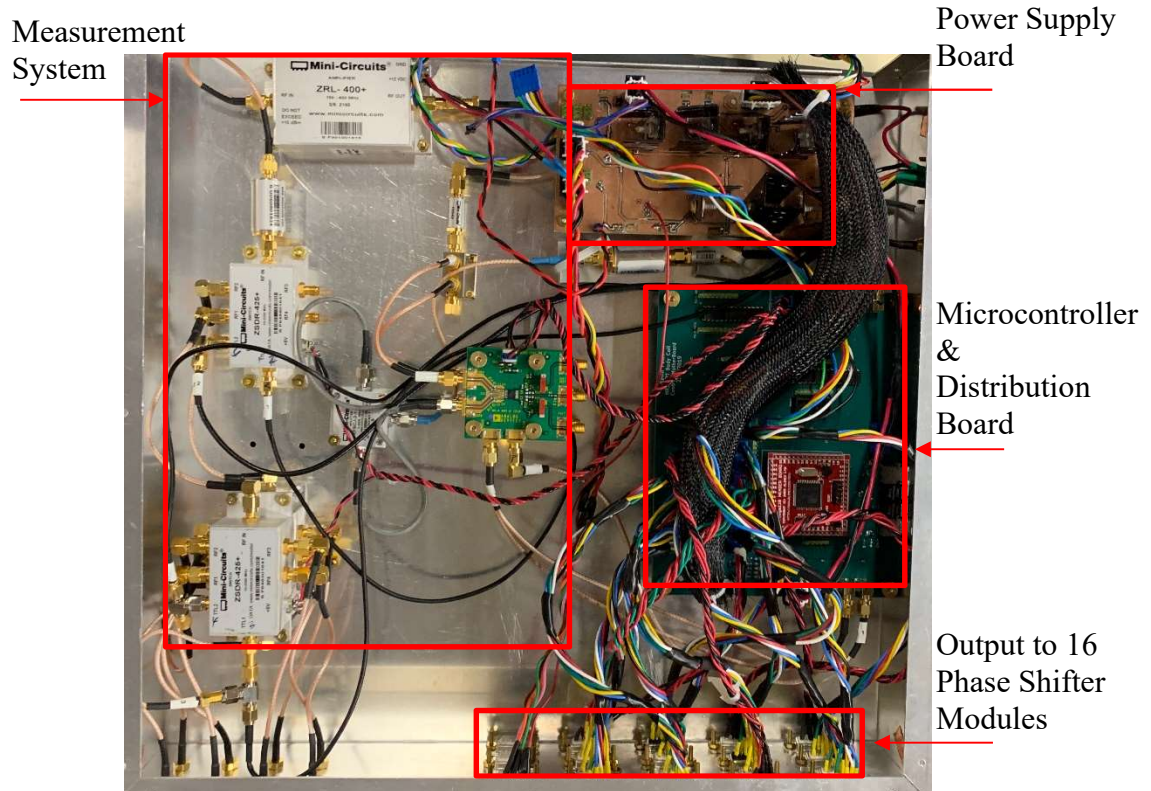


Figure 3.11 – Controller layout which houses the power supply board, measurement system, and microcontroller

3.3.1 Fiber Optic Communication

In order to avoid electromagnetic interference between the controller uses fiber optic cables for communication. Using the fiber optic lines communication system is isolated from the magnetic field which could possibly contaminate the message. The fiber optic messages between the BeagleBone Black and MCU by sending an asynchronous UART message with a baud rate of 1MHz. The UART message is sent between connecting the Rx and Tx port between two devices that both support UART encryption. Once the port is connected communication between the devices is very simple as it only requires writing messages encrypted within 1 byte.

The message is encoded in a one-byte message, in which the first two bits determine the type of command and then further decisions can be made depending on the next few bits, this form a decision. The fiber optic commands were allocated in order to get the most throughput by compacting as many controls in one command. Table 3.2 lists all of the messages used between the MCU and the BeagleBone.

Messages for BBB to MCU									
	Hex	bit 1	bit 2	bit 3	bit 4	bit 5	bit 6	bit 7	bit 8
ADC	0xC0 - 0xC7	1	1	0	0	0	Channels [0-7]		
Error	0xC8	1	1	0	0	1	0	0	0
Heartbeat	0xC9	1	1	0	0	1	0	0	1
Wakeup	0xCA	1	1	0	0	1	0	1	0
Sleep	0xCB	1	1	0	0	1	0	1	1
Clear MCU memory	0xD0	1	1	0	1	0	0	0	0
Compact MCU	0xD1	1	1	0	1	0	0	0	1
Store flag on	0xD2	1	1	0	1	0	0	1	0
Store flag off	0xD3	1	1	0	1	0	0	1	1
Dynamic mode on	0xD4	1	1	0	1	0	1	0	0
Dynamic mode off	0xD5	1	1	0	1	0	1	0	1
LSB Phases Shifter	0x80 - 0xBF	1	0	Channel[0 -7]			22.5	45	90
Expansion Chips 180/50	0x40 - 0x7F	0	1	180/50	[1-4]/[5-8]	C1/5	C2/6	C2/7	C2/8
Expansion Chips SD/SP	0x00 - 0x3F	0	0	1	[1-4]/[5-8]	C1/5	C2/6	C2/7	C2/8

Table 3.2 – Byte codes for the messages sent over the fiber optic Lines

3.3.2 Controlling the Phase Shifters

The phase shifter is completely TTL based making controlling the state very simple as it only requires setting a digital I/O high or low based on the necessary state. Each channel is designed to have five bits of control on the phase shifter. Therefore, a total of 40 control lines are needing. Due to the lack of GPIO pin on the MCU additional control lines were placed using the MSP23S17 GPIO expansion chip. These expansion chips are controlled by an SPI interface and add an additional 16 Digital I/O.

The phase shifter as well requires a large amount of power, 600mA of 5V and 20mA of -48V. Due to high current power being moved from a long distance the 7.5V source is not a reliable reference as there is will be a large voltage drop, therefore, the DC power is filtered and regulated down using an LDO voltage regulator. Fortunately, the current load for -48V is not very high, therefore, it only requires a low pass filtering and not a voltage regulator.

3.3.3 Dynamically Controlling the Phase Shifters

In order to accommodate multi-slice applications for using the system with more complicated pulse sequences, this required the system to be able to change the state of the phase shifter per RF pulse. This requires that the system is triggered by the MRI scanner for every RF pulse and will then change states dynamically from a list of shim solutions. While this could be performed by sequentially going through every channel and setting the phase shifter by telling the system to do so using the fiber optic lines, but this would operate in the order of 200ms. In order to operate the system much faster a different way of the method in setting the phase shifters.

Dynamic shimming was performed using the onboard memory of both the BeagleBone and microcontroller to store shim solutions per slice. After shim solutions are indicated on the GUI the data is transferred over to the BeagleBone Black which then flags the microcontroller to operate in Dynamic mode. Once microcontroller has been placed in Dynamic the Beaglebone will spam all of the shim solutions over fiber optics and then place the microcontroller to sleep. The Beaglebone will then wake up the microcontroller

to set the shim solution and then put it back to sleep. The BeagleBone is triggered by using the RF amplifier's unblank signal to indicate to prepare for the next shim solution. In order to adapt BeagleBone to scanner additional glue logic made of a series of logic gates and a 5V – 3.3V logic converter. This method has proven adequate for dynamic solutions being able to switch between shim solution in less than 10ms.

In order to accommodate scenarios where the same shim solution is applied to the entire TR and every RF pulse. The system was programmed to be able to count the amount of RF pulse before changing to the next shim solution. This is very useful when doing pulse sequence such a spin-echo that requires the same shim solution for the 90° and 180° pulse. Using this method the system will count that N RF pulse have occurred and tells that to change the shim solution for the next TR.

Using this method, the system is only limited by the memory size of the microcontroller in terms of how many shim solutions can be saved and cycled through. If more shim solutions are required it is solely a matter of adding additional memory to the ATMEL128. The system has been tested in the lab to cycle through a maximum of 125 different shim solutions, but this is more than enough for most pulse sequence. The switching speed using was found to be less than 10ms. Figure 3.12 shows that after a trigger is applied to the system 7.9ms later all of the phase shifters will change states. While Figure 3.12 does show some instability after switching this is a sampling artifact from the oscilloscope.

This data was taken by simply looking at the field inside of the liquid phantom change measured by using a cross probe connected to an oscilloscope. The data was

acquired by switching between two different shim solution generated with a power difference of 14.5dB or a power ratio of 28.1. Figure 3.13 and Figure 3.14 were acquired in a similar manner but using different shim solutions with the system counting for one and two triggers before changing shim solutions. Essentially Figure 3.13 resembling the

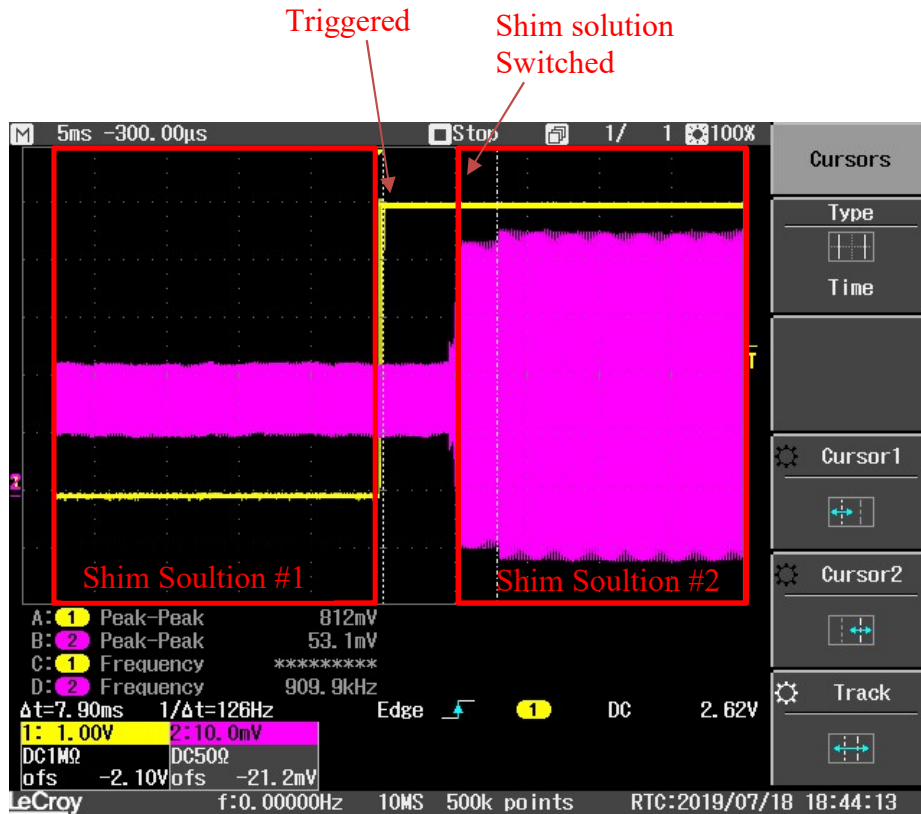


Figure 3.12 – Timing of phase shifting being applied dynamically due to an external trigger

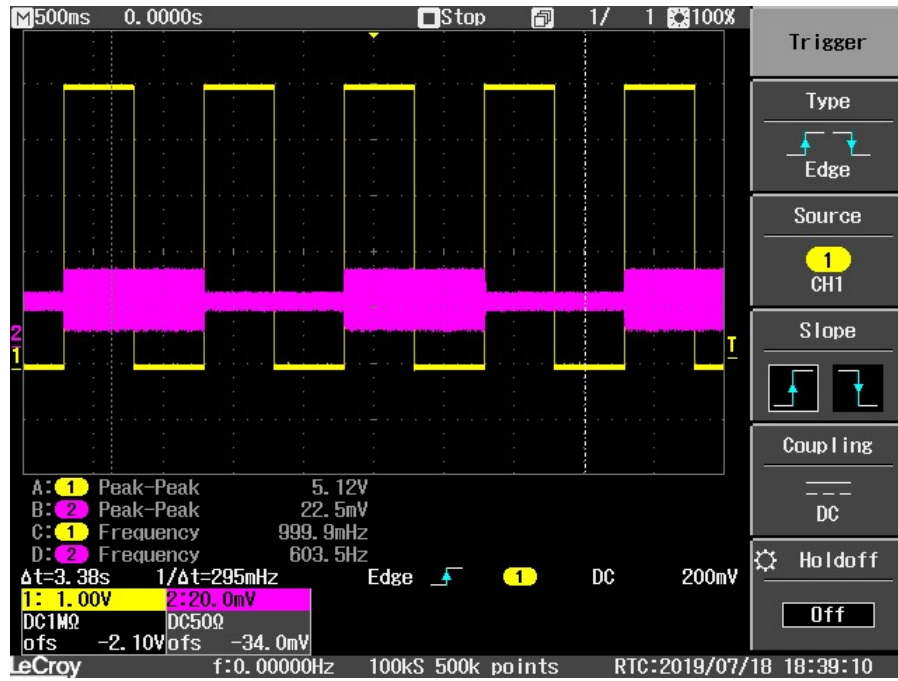


Figure 3.13 – Phase dynamically shifting after one trigger is applied

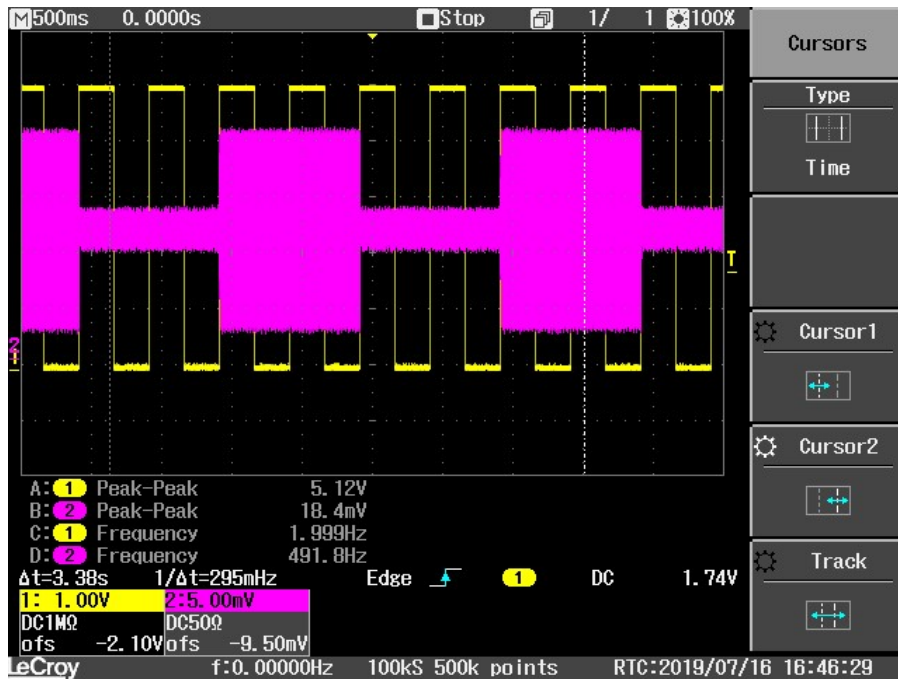


Figure 3.14 – Phase dynamically shifting after two triggers are applied

3.3.4 In-Phase/Birdcage/Anti-birdcage Mode

The system additionally has the ability to compensate for the natural phase nonlinearity of the whole system due to the inaccuracy of the phase shifters, cables lengths, or dipole placement. This is performed by simply using the measurement system to read the phases on each dipole element when a zero-phase shift is applied. The system will then apply the nearest conjugate phase shift that was read for every channel. Doing so will get the system as close to 0° phase difference per channel with a 22.5° resolution.

Furthermore, the system takes advantage of the In-Phase feature in order to set shim solutions as birdcage and anti-birdcage mode. After applying the In-Phase function the system will then create by Birdcage or Anti-birdcage pattern by simply adding $[0, 45, \dots, -90, -45]$ or $[-45, -90, \dots, 45, 0]$ respectively to the offset phase calculated to create In-Phase.

3.3.5 Active Transmit/Receive Switches & Pin Diode Driver

The last element of the controller is the active Transmit/Receive(T/R) switches were built by others in the lab and a two-channel pin diode driver that to switch the state of the T/R switches between transmit and receive mode. The pin diode driver is directly connected to the TR switches and designed to be controlled from the MRI scanner's RF amplifier unblank trigger. The pin diode driver is designed to output 1.2A at 5V in transmit mode, while in receive mode is capable of outputting 20mA at -48V.

The pin diode driver is designed by using a simple topology of stacked PNP transistors in conjunction with bootstrapping resistors. The top stage is conducting in

saturation mode for forward bias (transmit mode), likewise, the bottom stage is used for reverse bias (receive mode). The circuit is controlled using a TTL signal that when it is high (or 5V) puts the top stage transistor in off position turning on the diode and therefore forcing the bottom stage transistor to allow the -48V to pass through. Additionally, the top stage takes advantage of a Darlington pair for necessary current output along with a speed up resistor to quickly discharge the parasite capacitance. A Schottky diode was chosen over the more common P-N junction diode for the lower junction voltage in forward bias and the faster switching speed. Figure 3.15 shows a schematic layout of the pin diode driver.

The pin diode driver is placed inside of a small box for shielding in order to prevent issues with electromagnetic interference (EMI) is shown in Figure 3.16. Additionally, when the trigger input for the pin diode is floating, EMI issues can cause it to output a voltage between 0 and 5V switching in the MHz range, but this can be prevented by filtering the input. Therefore, a bullet Mini-Circuits low pass filter(BLP-21+) with a cutoff frequency of 21MHz is placed and a shielded RG – 316 sma cable is used to connect the filter to board. The pin diode driver is capable of outputting 650mA over a single channel and 1.3A using both channels. The board is able to switch between transmit and receive states in less than 1 μ s. Similar to the input the output is connected through an RG-316 SMA cable for shielding to prevent EMI.

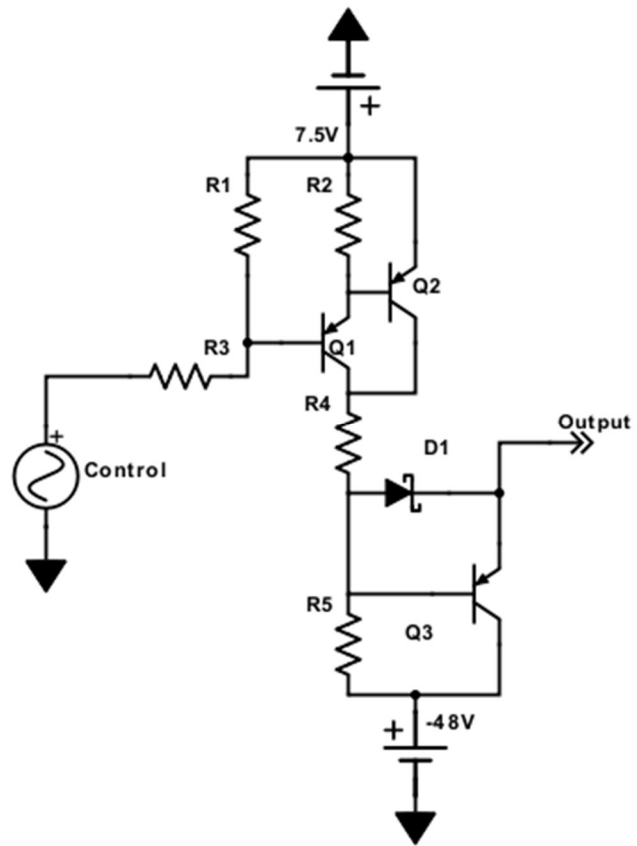


Figure 3.15 – Schematic for a 1 Channel pin diode driver using the designed topology

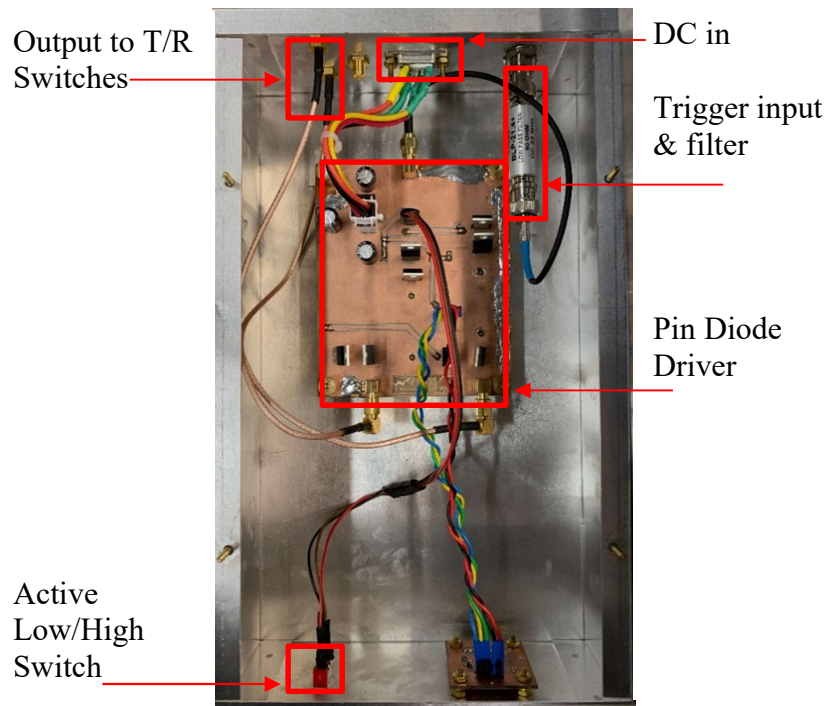


Figure 3.16 – The constructed 2 Channel Transmit/Receive pin diode driver

CHAPTER IV

REMOTELY MEASURING GAIN & PHASE

In order to remotely measure the phase shifter's ability to change phase for functionality a subsystem that can remotely measure gain and phase was needed. This subsystem is designed to make checking the functionality of phase shifter without requiring additional equipment that may be cumbersome to access within the magnet room such as a Vector Network Analyzer (VNA). Using the current probes placed on the coil the applied to transmit phase and power on each individual channel can be measured. The system as well can use these measurements as a form of feedback for checking of system functionality. For simplicity, the system is designed to be operated remotely from inside the control room, without the need to remove eight cables outside of the magnet room, but still acquire measurements from inside the magnet's bore. The Analog Devices 8302(AD8302) evaluation board was chosen for calculating gain and phase. Lastly, the measurement for this system is only operated at 298MHz but could easily be modified to work at other frequencies for a different application.

4.1 Using the AD8302 Evaluation Boards

A single AD8302 can calculate the gain and absolute value of the phase between an RF signal and a reference signal of the same frequency between power levels of -60 to 0 dBm. The absolute value of phase is given as from 0° to 180° corresponding to a DC voltage between 0V to 1.8V in order get. Therefore, a phase difference of 1° results in an

output change of 1mA. In this application, the reference signal was generated using the TPI (frequency synthesizer) that was kept at a constant frequency, phase, and amplitude. This reference signal was not of much importance, but solely required to operate at arbitrary sinusoidal RF signal at 298MHz as all the measurements acquired would all be reference gain and phase on channel one of the coils.

Using a single AD8302 board gives the absolute value of the phase difference between the signal of interest and reference signal. Figure 4.1 shows an illustration of the expected output of the phase shift between 0° to 360° resembling a triangle. At 180 degrees this is the bottom of the triangle or minimum detected phase difference shows that output phase value from AD8302 is between 0V to 1.8V or 0° to 180° . Furthermore, after a phase difference of 180 degrees input phase difference increase the detected phase difference decreases as linearity showing that the output is the absolute value of the input phase difference.

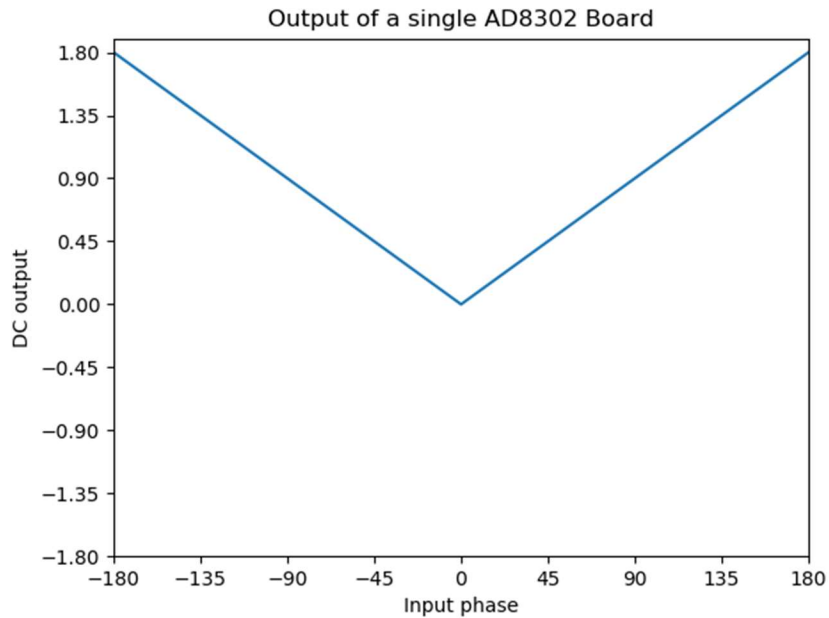


Figure 4.1 – Phase output of a single AD8302 evaluation board

In order to get full range phase difference from -180° to 180° (or 0° to 360°), two of AD8302 evaluation boards can be used in order to determine what the total phase difference. The hardware setup is so that two AD8302 evaluation boards have the same reference signal but different phase signals. The evaluation boards are set up so that using a hybrid coupler the signal phase input into the second AD8302 evaluation board is used so that the input signal is identical but lagging by 90° . Using this setup, the output of both AD8302 evaluation boards will differ by an output of 90° , this then creates four bins which can be used to decode the full range phase value. This setup is shown in Figure 4.2.

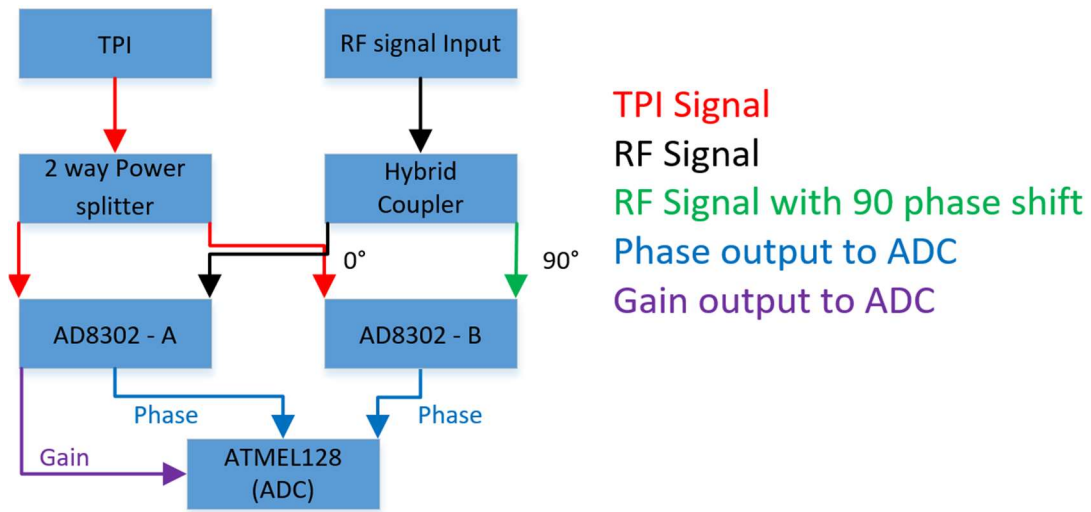


Figure 4.2 – Hardware setup of the measurement system

Figure 4.3 illustrates that once a 90° phase shift is applied the output of the two evaluation boards has four distinct bins that they can be used to decode the true phase difference. Looking at the four bins the case structure in equations 4.1 – 4.11 can be used to read the true phase of the input signal.

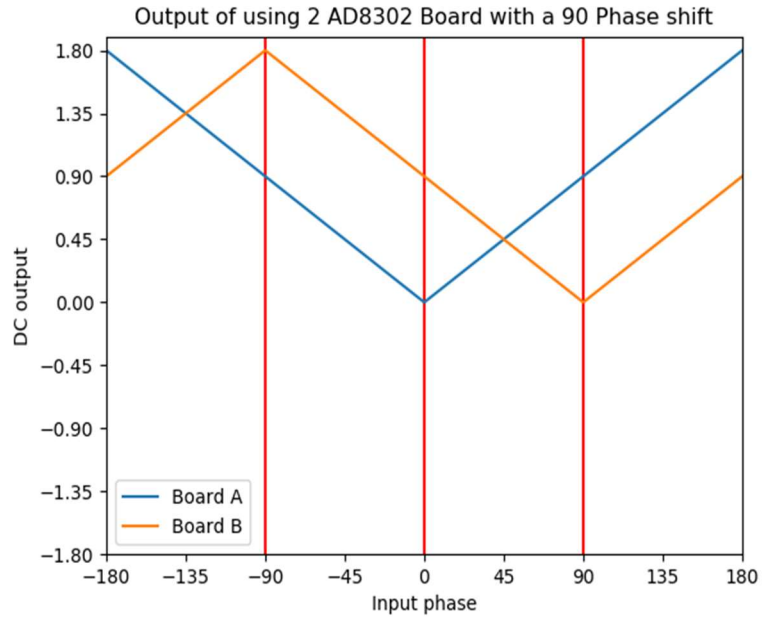


Figure 4.3 – Phase output of using 2 evaluation boards with a hybrid coupler

By checking the 4 bins shown sequentially it is possible to decode the true input phase difference from digitized voltages read from AD8302 boards using the ADC on the Atmel128 MCU. Once the output has been digitized and ADC values have been converted to numerical value a simple script can be written using case structure from that true phase from -180° to 180° will be read from the output of the python program.

$$\mathbf{Vref = 1.8} \quad (4.1)$$

$$\mathbf{If } eval_a \geq (.75 * Vref) \mathbf{ and } (eval_b \leq .5 * Vref): \quad (4.2)$$

$$\mathbf{Phase = -1(eval_b - .9)100 + 0} \quad (4.3)$$

$$\mathbf{Else if } (eval_b < .25 * Vref): \quad (4.4)$$

$$\mathbf{Phase = -1(eval_a - .9)100 + 90} \quad (4.5)$$

$$\mathbf{Else if } (eval_a \leq .25 * Vref): \quad (4.6)$$

$$\mathbf{Phase = (eval_b - .9)100 + 180} \quad (4.7)$$

$$\mathbf{Else if } eval_b > (.75 * Vref): \quad (4.8)$$

$$\mathbf{Phase = (eval_a - .9)100 + 270} \quad (4.9)$$

$$\mathbf{Else If } eval_a \geq (.75 * Vref) \mathbf{ and } eval_b \geq (.75 * Vref): \quad (4.10)$$

$$\mathbf{Phase = 1(eval_b - .9)100 + 0} \quad \mathbf{(4.11)}$$

While the above the case structure could have been implanted using hardware or software. A hardware approach using the case structure would require using a collection of Operational Amplifiers (Op-Amp) in comparator and summer stage until the case structure is implemented with a single output and a single ADC. For simplicity and to reduce the required hardware this was implemented in a python program, but it required the use of two ADCs. After applying, the case structure above will output the true phase of the signal between 0° and 360° , but in order to get the value between -180° and 180° it required the following case structure.

$$\mathbf{If\ 180 < phase:} \quad \mathbf{(4.12)}$$

$$\mathbf{Phase = Phase - 360} \quad \mathbf{(4.13)}$$

$$\mathbf{Else\ If\ phase < -180:} \quad \mathbf{(4.14)}$$

$$\mathbf{Phase = Phase - 360} \quad \mathbf{(4.15)}$$

The output of using both case structures results in the real phase of the signal between -180° and 180° . Figure 4.4 is illustrating that the output of the decoded phase, but for simplicity, the phase is shown off by a factor of 100 in order to keep the values between -1.8 and 1.8 in order to compare with the inputs of the case structure.

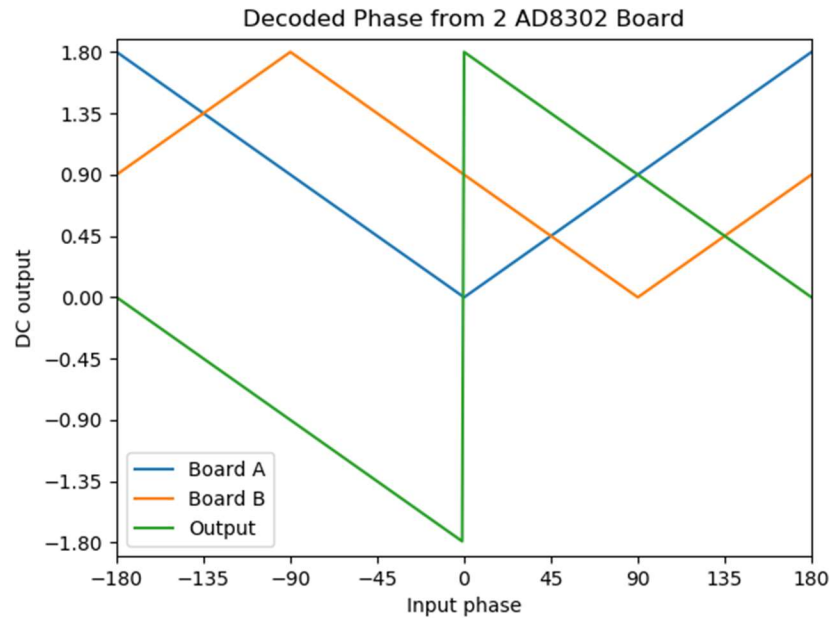


Figure 4.4 – Phase output of the measurement system once the phase has been decoded

The gain was extracted from a single AD8302 board as the gain difference output solely differed by a factor .0295. Similar to the phase output the gain outputs are digitized using an ADC and those converted to a number that the equation could be applied to in software.

$$Gain(dB) = .0295 * V_{out} \text{ from AD8302} \quad (4.16)$$

4.2 Adapting the AD8302 For This System

In order to correctly use the AD8302 evaluation board to measure Gain & Phase remotely using and using Analog to Digital Converter (ADC) on the Atmel128 MCU to

measure on all eight channels required external hardware. A switching matrix was constructed using three digitally controllable 4x1 RF switches were used in order to allow 8 signals to connect to the phase measurement system and then digitally control which channel was being measured. A high pass filter and power limiter are placed in series cascaded directly after the switching in order to keep the signal within required power level and as well. The high pass filter is used in order to remove any RF frequencies below 290MHz for very aggressive filtering of any signal leaking from the gradient amplifiers. The current limiter was placed in order to prevent excess power from damaging the preamp and AD8302 board. A gain stage in the form of a preamp was then cascaded after the current limiter in order to increase the signal intensity well above the noise floor to preserve signal integrity. The preamp was placed directly before switching matrix in order to accommodate all eight channels but only require a single Preamp. Lastly, a hybrid coupler is used in order to divide the RF power into two ports and generate a 90° phase shift on one port to get full range phase shifting on a single channel. The entire signal chain is illustrated in Figure 4.5.

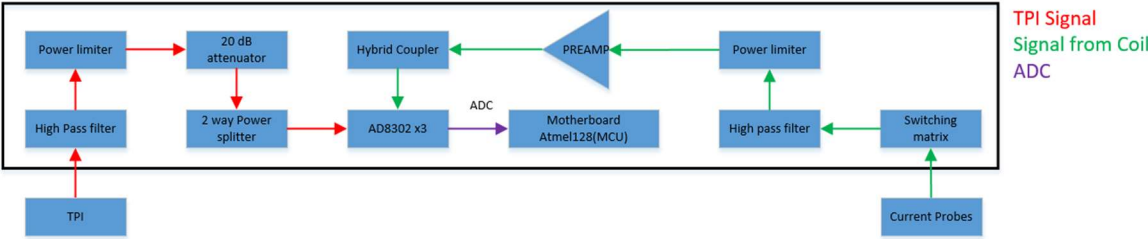


Figure 4.5 – Signal chain of the measurement system

4.3 Using the Measurement System

This subsystem is operated by simply connecting both of the 3.2W RF amplifiers directly to the two 1x4 Wilkinson power splitter in the system rack and connecting the eight current probes from the coil to the switching matrix on the controller. The rest of the system is not altered in order to allow to do full system gain and phase measurements.

The measurement system, when compared to the VNA on average, has an average phase difference of 5.48° (or 1.522%) with a maximum error of 13.81° (or 3.836%). Furthermore, the standard error mean was found to be only 5.48° (or .303%) this should the error is typically very close to the average error and not the maximum error. Figure 4.6 shows the measurements acquired from the measurement system along with error bars comparing to the VNA measurements. For validation of the system, the measurements were taken using the entire transmit path using both of the 3.2W RF amplifiers and then measuring the signal on the current probes on the dipoles. Considering the resolution of the phase shifters is only 22.5° the maximum error of 13.81° is not considered significant. Ultimately the measurement system was found to be capable of detecting wither a phase shift was successfully applied onto the coil.

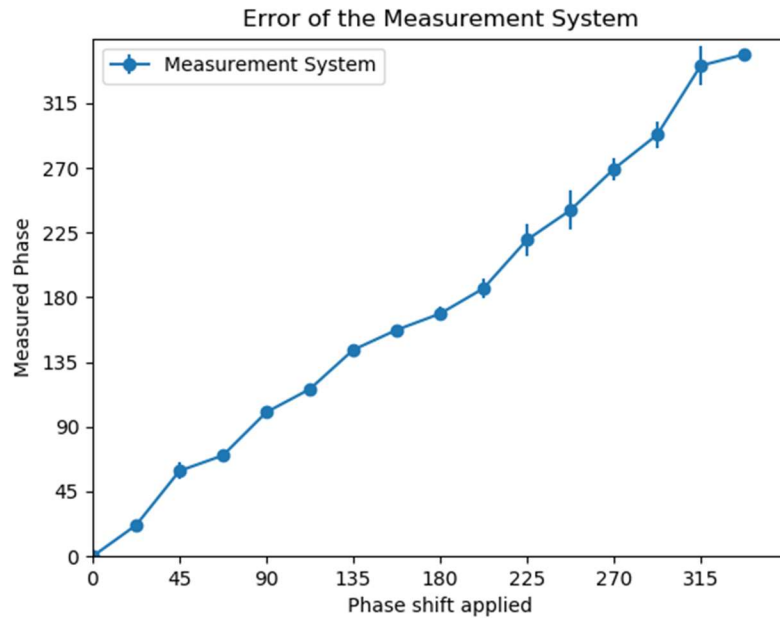


Figure 4.6 – Accuracy of the measurement system compared to the VNA

4.4 Noise Mitigation

In order to acquire accurate measurements from the system, the system required the ability to suppress noise from the environment and acquisition. Due to the nature of pulse sequences being used in the 7T MRI suite the gradient transmitted very high power. Due to poor shielding of the control units and cables, electromagnetic signals could potentially get coupled in. Other issues arose from the AD8302 boards have 250mV of noise floating on top of the actual signal. The noise of evaluation boards makes it very difficultly to make reliable measurements.

In order to suppress the noise from the gradient pulse entering into the control system required filtering out any undesired frequencies. The first step was to place filters on after the switching matrix(for the current probes) and 1-2-way power splitter(reference

signal from the TPI). For this purpose, mini-circuits low pass filters with a cutoff frequency of 290MHz were chosen. This filter was specifically chosen as the gradient would have a frequency much lower than 290MHz, therefore, leaving only other frequency left would of 298MHz(which is the desired frequency for this application). As well the filters were statically placed so that only 2 filters were required as opposed to 9 filters that would be required if one was placed at every rf input of the control unit. The second step to filtering out any gradient noise was to place a wire mesh around every cable that contained any sort signal. The wire mesh was soldered to ground on both of connection in order to trap the signal within a ground plane preventing any interference from outside sources as shown in Figure 4.7.

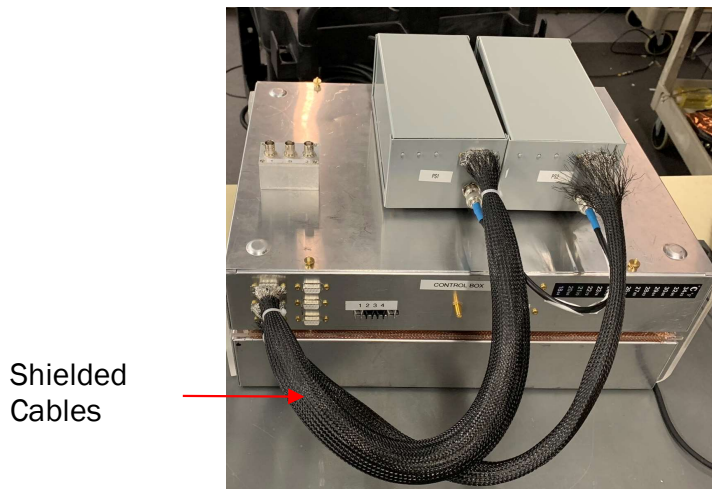


Figure 4.7 – System connected for a signal channel using built shielded DE9 cables

In order to filter out any noise coming from the AD8302 evaluation board, a simple RC filter was used. The capacitor was used in parallel with the output resistance of the

AD8302 boards. In order to measure the output resistance of the gain and phase a shunt resistor was used in order to calculate the output resistance. First, the output current is calculated by using the difference in the voltage of when it left open and loaded to a 50Ω resistor and then dividing by the shunt resistance.

$$I_o = \frac{V_{open} - V_{Shunt}}{R_{Shunt}} \quad (4.17)$$

The output resistor is then simply the product of voltage at open circuit and the output current.

$$R_{out} = V_{open} * I_o \quad (4.18)$$

This process led to finding that the output resistance of the gain port was $.44385\Omega$ and for the phase output is $.05413\Omega$. For simplicity, both of the output resistances were approximated to $.5\Omega$ to account for measurement error and simplicity. The next step is to find the value of the capacitor using the output resistance of the evaluation board and the desired time delay. The maximum sampling rate of the ADC on Atmel128 is 8MHz so that will be used to find the necessary capacitance.

$$t = R_o C \quad (4.19)$$

$$f_s = \frac{1}{t} = \frac{1}{R_o C} \quad (4.20)$$

$$C = \frac{1}{R_o f_s} = \frac{1}{.5 * 8 * 10^6} = 250nF \quad (4.21)$$

This ultimately led to finding that a 250nF capacitive was necessary to filter out the noise and maintain the speed of the ADC. Unfortunately, a 250nF capacitor was not easily obtainable in a nonmagnetic package so a 160nF capacitor had to be used. While this does will not cause timing issues due to using a lower capacitive there will still be a sufficient

amount of noise after the filtering. After the filter capacitor, 50mV of noise was still present this was dealt with by averaging. This process of shunting the output is further illustrated in Figure 4.8

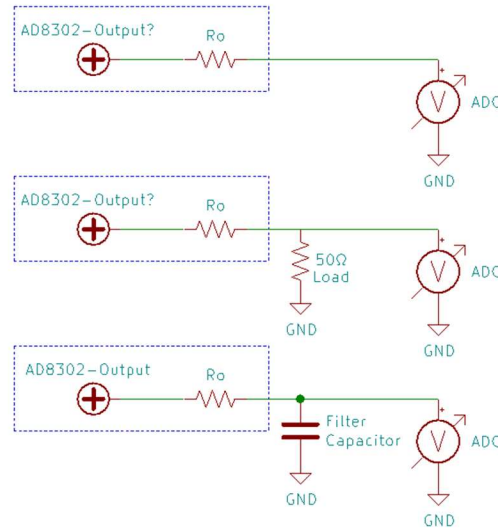


Figure 4.8 – Process for finding the appropriate filter capacitor for the AD8302 evaluation board

Averaging on the system is performed on the client end of the system. The default number of averages is 32 in order to perform accurate measurements overall cases including when lower RF power is used. The number of averages was found by checking the measurements for repeatability. A test script was written that takes two states averaged measurements on all eight channels and switching through all 17 states of the phase shifter individual for a total of 136 measurements. The fluctuation in measurements was found by finding the difference in the two measurements. The average fluctuation for all of the measurements was found to be 3° (or .833%).

4.5 Broadband Operation

The measurement system could easily be modified to work at other frequencies for testing of different coils. Currently, the measurement system is only operated at 298MHz for water at 7T. Currently, the system is configured to work only near the frequency of interest(298MHz) resulting in the frequency range of 290 MHz (high pass filter) to 400MHz(preamp) resulting in 110MHz bandwidth. Table 4.1 shows the different frequency ranges for all of the devices in the measurement system. If a wider bandwidth is needed it would simply be changing the devices. If a lower frequency between 220MHz to 290MHz is needed it requires simply changing the high pass filter to have a lower cutoff frequency. Once the High pass filter is changed the next limiting factor is the Hybrid coupler, so this will have to be changed afterward for one with range lower frequency is desired, but this would result in a frequency range of 150MHz to 400MHz. Similar this can be done for the upper-frequency limits, but this much as frequency limits are more widely distributed. Figure 4.9 shows the location of the components throughout the measurement system. Due to the AD8302 being the heart of the measurement system the maximum frequency band will be 0Hz to 2700MHz. The AD8302 will not be able to make any measurement outside of this bandwidth and will require additional hardware to shift a higher frequency within the operating range of the evaluation board.

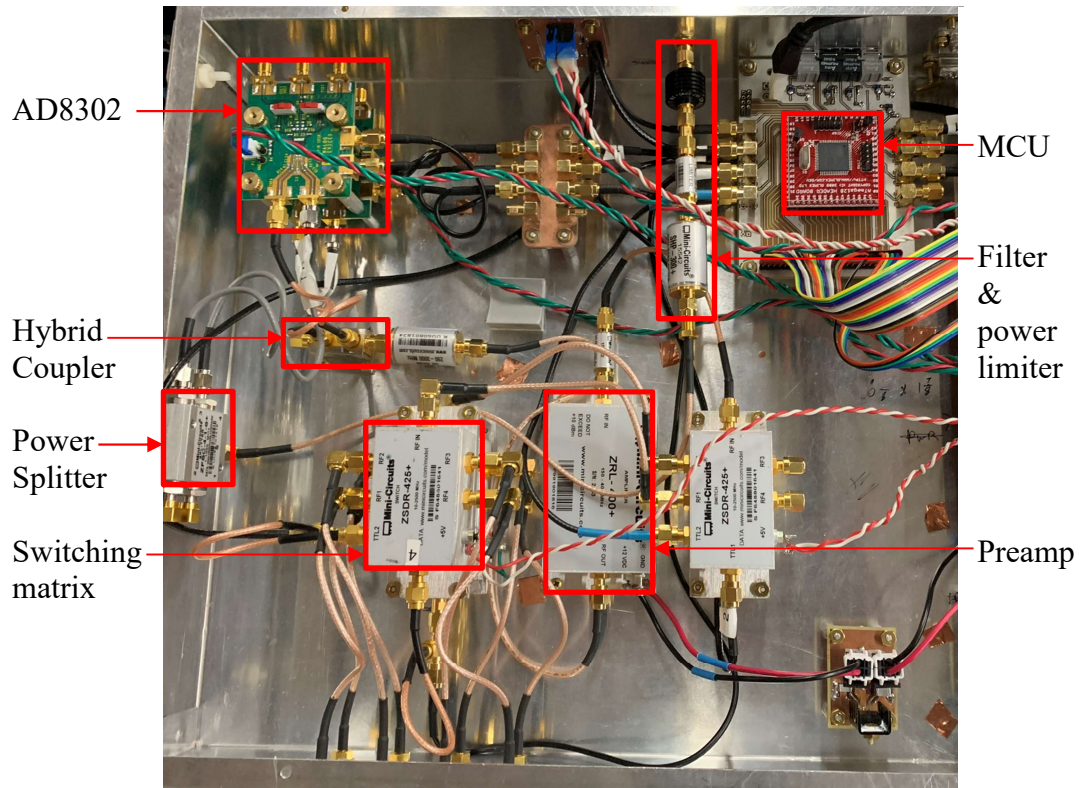


Figure 4.9 – Measurement system components placed inside of the controller

Item	Supplier	Device	Low frequency (MHz)	High frequency (MHz)
High Pass filter	Mini-Circuits	SHP-300+	290	~
90° Hybrid coupler	Mini-Circuits	ZX10Q-2-3-S+	220	470
Preamplifier	Mini-Circuits	ZRL-400+	150	400
2-way Power splitter	Mini-Circuits	ZFSC-2-1-S+	5	500
Power Amplifiers	Sodial	Ham radio amplifier	1	700
RF Mux	Mini-Circuits	ZSDR-425+	10E-6	2500
AD8302 Evaluation Board	Analog Devices	AD8302	~0	2700
Frequency synthesizer	RF – consultant	TPI -1001-B	35	4400
Power limiter	Mini-Circuits	VLM-73-1W-S+	30	7000

Table 4.1 – Frequency bands of the components used in the measurement system

CHAPTER V

EXERCISING THE SYSTEM AS A WHOLE

The system as a whole has been developed to perform beam steering(B_1 steering) which is focusing energy at a point of interest in order to generate an adequate B_1 . This is performed by changing the phase on each channel of the coil. In order to move the focused energy to a different location, a different set of phase shifters(phase solution) is required. This is different than B_1 shimming which the process of increasing the homogeneity of the RF field. B_1 shimming would, in turn, require shim solutions. In this thesis, the terms B_1 shimming and shim solution will be used as they are more common in literature.

5.1 Testing with the Positioner System

For testing of the system in the lab at MRSL the positioner system originally built by Jeff Boyer in 1995 was used for testing of this system in the lab at MRSL [21]. The system basically is two stepper motors that move a cross-probe (two magnetic fields pick-up probes placed perpendicular to each other) across the phantom. The probe is then connected to a hybrid coupler in order to combine the magnetic fields B_x and B_y field into $B_x + jB_y$ and $B_x - jB_y$ is then connected to the VNA in S_{21} mode for measuring the gain and phase [22].

For this application, the positioner system was retrofitted to scan across the almond-shaped liquid phantom is shown in Figure 5.1. This system was used in order to verify the functionality of the system and as well as the imaging that would be conducted

at UTSW. Ideally using this system, the B_1 mapping, and shimming process should resemble the same field pattern that can be acquired off the 7T scanner at UTSW.

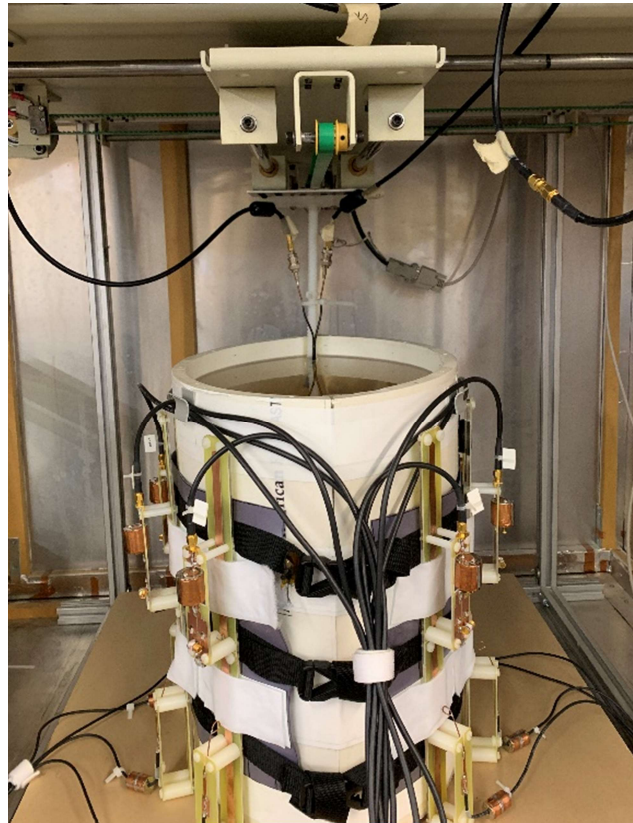


Figure 5.1 – Positioner system being used with the liquid phantom

Connecting the positioner system to the developed control system is relatively simple and is illustrated in Figure 5.2. The first step is to place the VNA in S_{21} mode and then connected the transmit port into the 4x1 power splitter in the RF amplifier unit by disconnecting the TPI. The two output ports from the power supply unit are connected to both of the high power – power splitter in the system rack. The coil must be placed around

the liquid phantom with a cross probe inserted into the phantom. The cross probe is then connected to the 0° and 90° ports of the hybrid coupler. Finally, one of the outputs of the hybrid coupler must be connected to a 50Ω load and other to the receive port of the VNA.

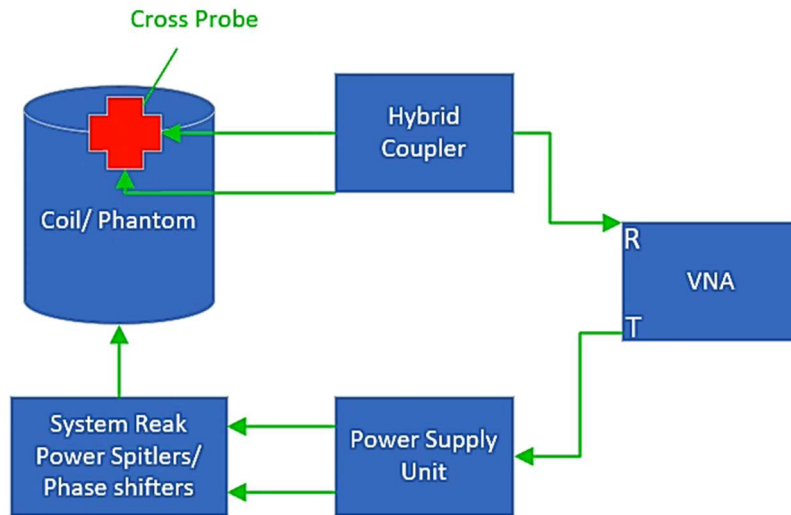


Figure 5.2 – Diagram of the positioner system setup with the developed body coil system

Using the positioner system can be done using two methods the first requires using a fixpoint and second requires collecting eight B_1 maps. The first method requires placing the cross probe is placed at the Region of interest of where to optimize the B_1 field. The control system is used to terminate seven of the eight channels. The phase contribution due to the single channel is read and recorded off of the VNA, this is then repeated for every single channel till eight phases have been recorded. The shimming process was done by finding the conjugate(or negative) phase of recorded values collected earlier and

is then applied on the respective channel using the phase shifters. Figure 5.3 shows this procedure step by step.

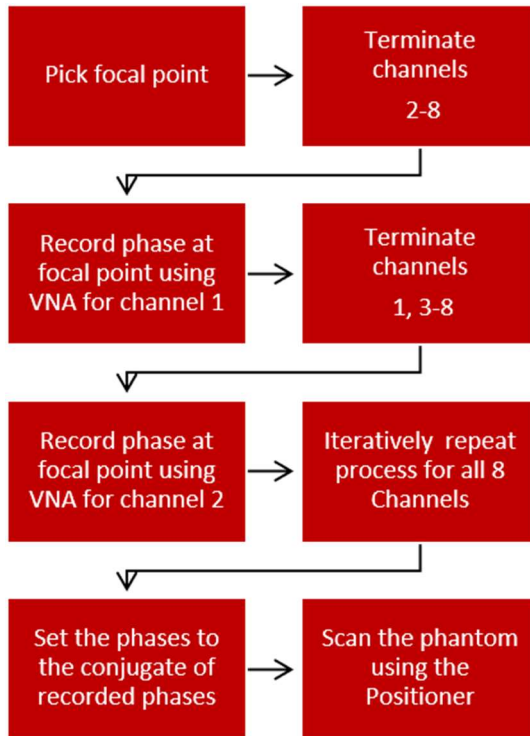


Figure 5.3 – Procedure for B₁ Shimming using the positioner system at a fixed point

The positioner system as well can be used to collect eight B₁ maps and then pulling the necessary phase information from there as shown in Figure 5.4. The same procedure of terminating seven of the eight channels is done in order to gather the phase contribution from each individual coil element. Once the phase is found for each individual channel the conjugate(or negative) phase is applied using the phase shifters.

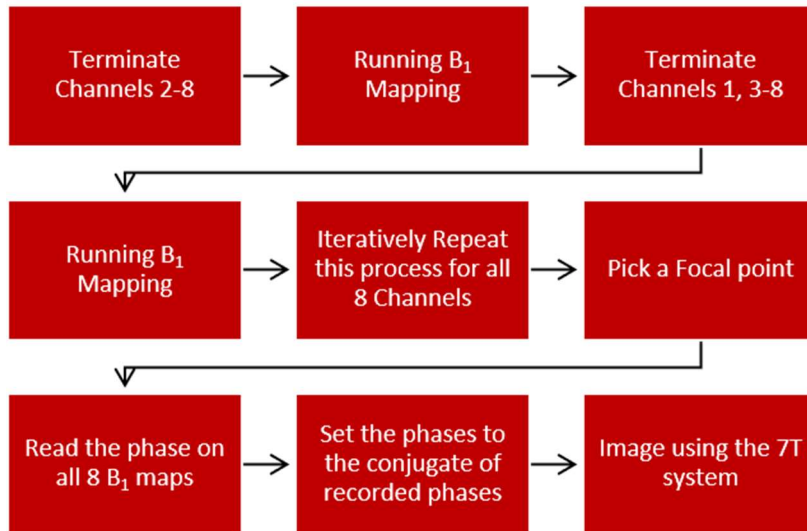


Figure 5.4 – Procedure for B₁ Shimming by collecting eight B₁ Maps

While both methods of using the positioner system can steer the beam and result in the same field pattern. The method of collecting the eight B₁ maps was used with the positioner system as that is done at UTSW.

Once the positioner has finished scanned the phantom it will save a CSV file on that contains data. The CSV file composes of 4 column vectors for the X coordinate, Y coordinate, Gain, and Phase. This data represents different images one for gain and the other for phase. In order to actually get the images out of the CSV file MATLAB program was written that will use convert the column vectors into actual images. The Matlab code will interpolate enough data points to get a high resolution image. The algorithm will then sort vectors into a 2D array in order to generate an image.

Simulations were done using Remcom and Matlab for changing of the focal spot. Various focal spots were tested, but the most interesting were deemed to be center, top, left and top left. Remcom was used to generate simulations of B₁ maps (consisting data

represent amplitude and phase) for all 8 coil elements over a human body phantom of the same size and shape built in the lab. The B_1 maps were then export to Matlab to apply the phase shift and preform the shimming process. The post-processing in Matlab is very much similar to experiments done with the positioner system. First, the phase contribution at a point is found for every individual coil element. The conjugate phase is then applied to the respective B_1 maps of the coil elements. Once the proper phase shifts have been applied the eight B_1 maps are summed to the shimmed imaged.

While generally, the dataset of interest is the magnitude image, but the phase data set has vital information. Phase maps can be used to determine if the beam was successfully steered and shows the exact region where the B_1 field is shimmed. The phase map can be useful when debugging. If the phase map does not show a homogenous region then the shim solution was not correctly applied. Overall a smooth phase shift resembles a homogenous region in the B_1 field, but a sharp phase break resembles inhomogeneity.

Table 5.1 shows the simulations done in the lab and then Table 5.2 gives the field maps collected using the positioner system. Both tables show the gain and phase of a few datasets collected to shim the transmit signals on the phantom. Looking at the table it can be seen that the patterns are almost identical. The scale factor for the images in Table 5.1 is 1cm to 6 matrix elements. The images in Table 5.2 have a scale factor of 1cm to 9 matrix elements.

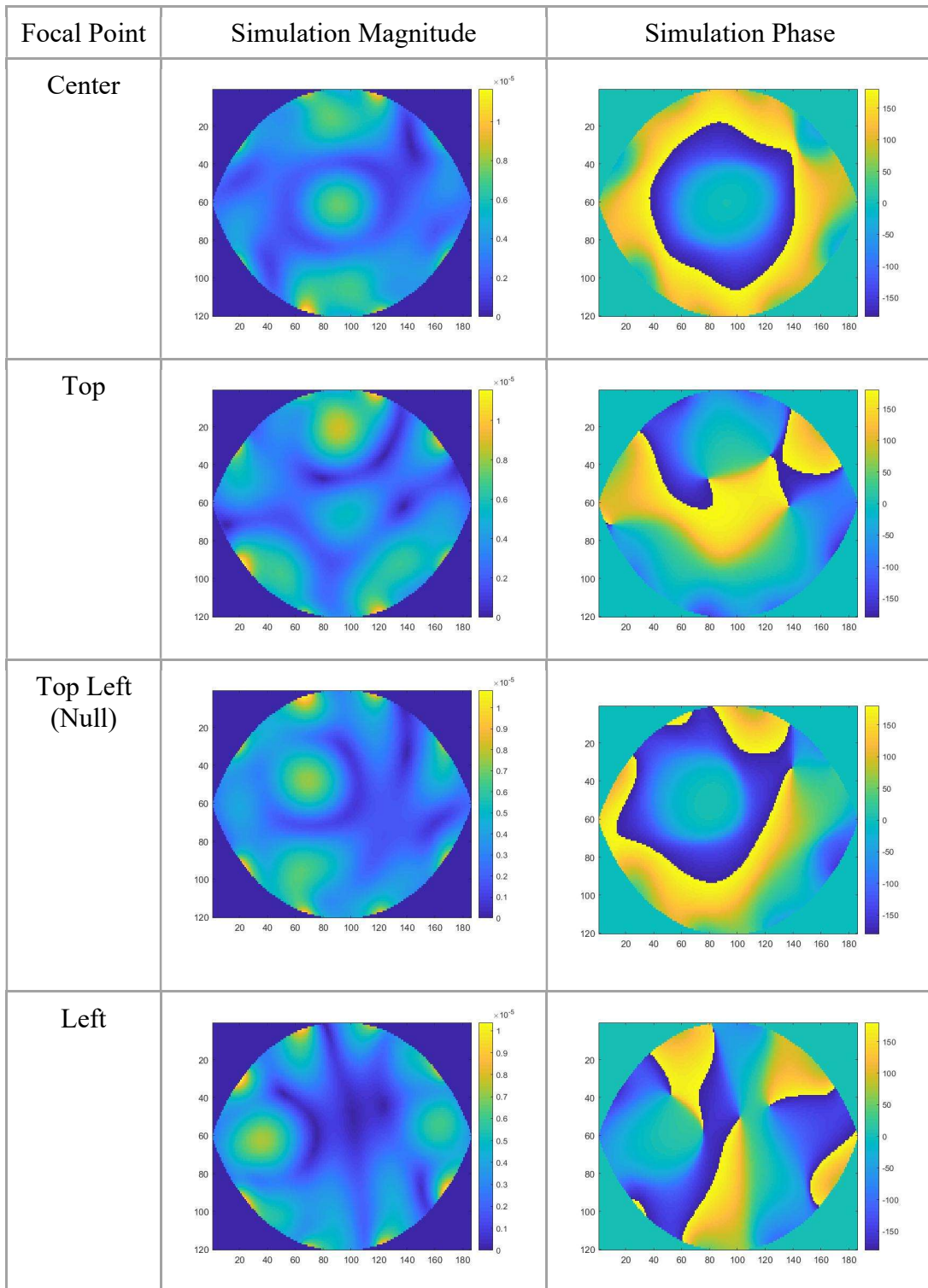


Table 5.1 – Simulations of B₁ Shimming at 4 different focal points

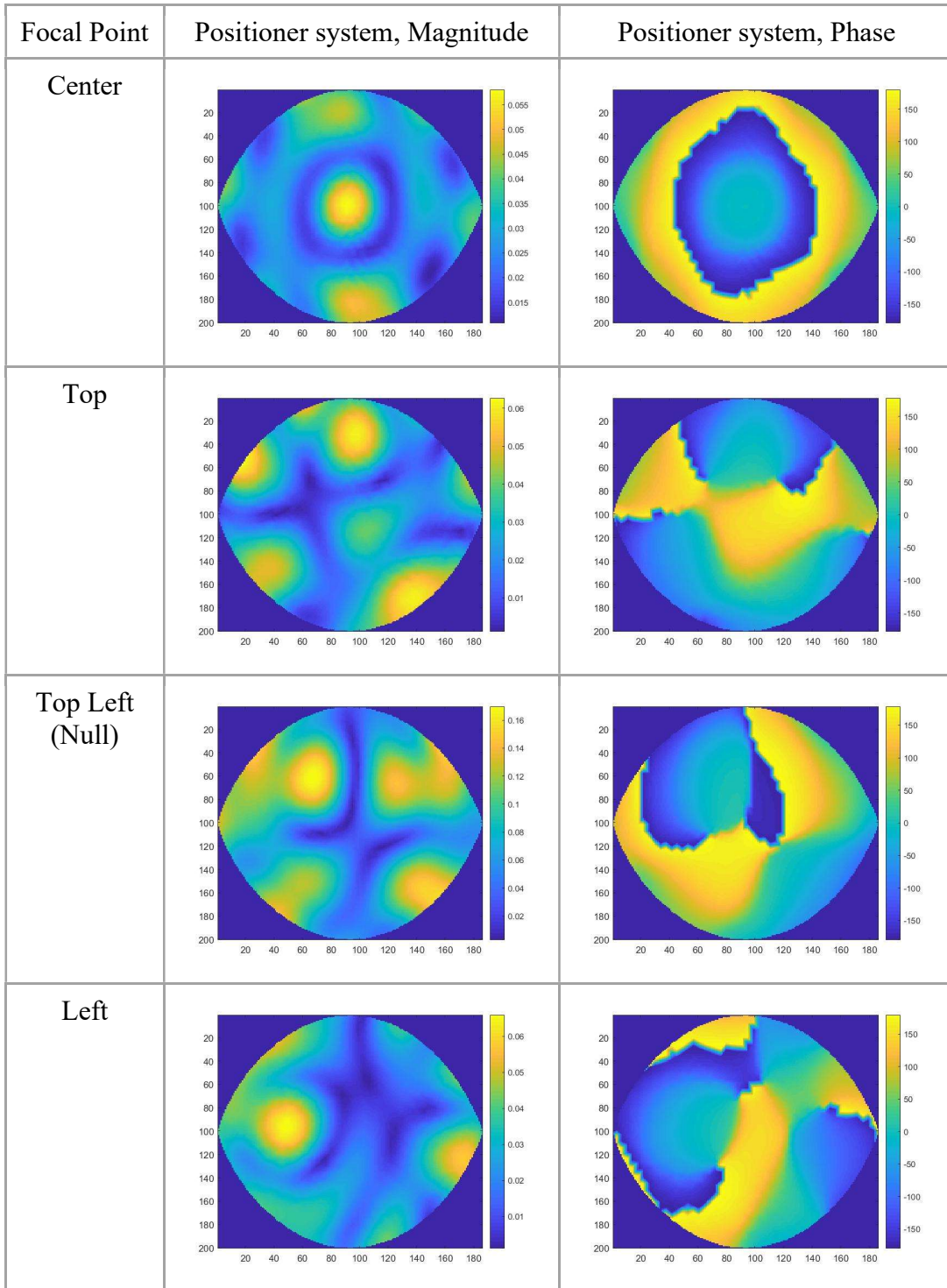


Table 5.2 – B₁ Shimming gain & phase field maps using the positioner system

5.2 Testing on the 7T MRI System

Testing on the 7T system was more perplexed due to the need of using very complicated pulse sequences for B₁ mapping and imaging, but the process of finding the shim solutions was very much similar to what was done in the lab using the positioner system using the method of collecting eight B₁ mapping. Phase information for B₁ mapping was actually acquired directly from the TR₂ images and B₁ mapping for the actual imaging process.

B₁ Mapping could have been by using a pulse sequence such as the Bloch-Siegert shift. This pulse sequence relies on the ability to apply an off-resonance RF pulse in order of a few kilohertz. Two Images are taken using different frequency shifts for off-resonance, where the images are then subtracted. The phase is then found to be proportional to the square of the magnitude of the resulting image [20].

The images below show that patterns from imaging on the 7T scanner seem to be very similar to the patterns from the positioner system. The issue here is that the images collected from the 7T scanner have more noise and show some small artifact, but this is most likely due to the pulse sequence or something with the scanner itself. The system was further tested in the lab to see if the noise or artifact would occur, but the issue did not occur again. Overall the general goal of being able to move the optimized region on interest during imaging on the 7T system in order to image different areas around the phantom was met. Table 5.3 shows the images collected from the 7T system for comparison with Table 5.1 and Table 5.2. The scale factor for Table 5.3 is 1cm to 3 matrix elements.

Unfortunately, B₁ Mapping process had a large amount of noise that it made finding shim solutions very difficult. Ultimately the system was able to steer the beam to the center, top, and top left, but not the left. Steering the beam to a focal point on the left was not possible, and there was not enough time to redo the B₁ Mapping with less noise.

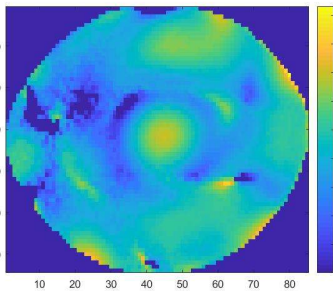
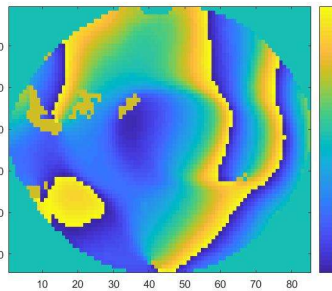
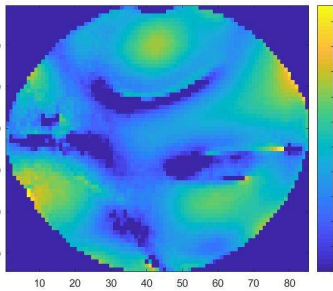
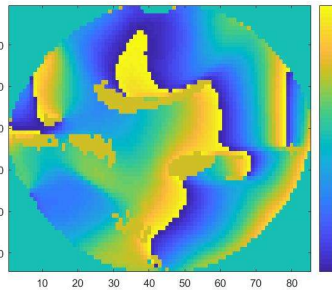
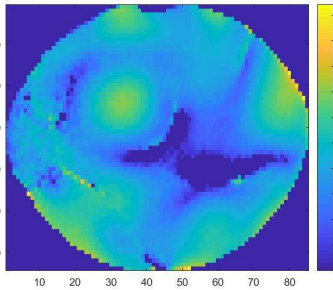
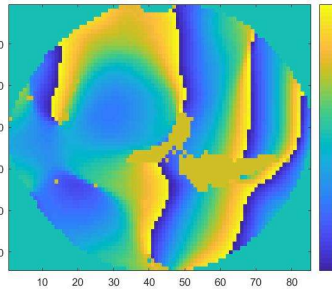
Focal Point	7T system, Magnitude	7T system, Phase
Center		
Top		
Top Left (Null)		

Table 5.3 – B₁ Shimming images using the 7T MRI system

CHAPTER VI

CONCLUSIONS AND FURTHER DEVELOPMENT

6.1 Summary

A Control System was built in order to dynamically control a set of digital controllable phase shifters for an eight-channel array for B_1 Shimming at 7T. The system as well can make gain and phase measurements for minor feedback and diagnostics. The system was tested on the 7T MRI scanner at the University of Texas Southwestern and using a positioner system in Magnetic Resonance System Lab at Texas A&M University. It was found that using the current method of dynamically shimming resulted be able to move between shim solutions in less 10ms. While this is sufficient for most multi-slice applications, but there is still quite a bit of latency that prevents the usage of more complicated pulse sequences. Most of the latency is due to the necessity of waking up the Microcontroller. Methods and preliminary work in order to speed up the control system are discussed in sections 6.2.

The system as well currently had the ability to support the power requirements of 16 phase shifter modules (8 low bits modules and 8 high bits modules) and eight active T/R switches. This resulted in a total current draw of 12.8A, but this is generally considered very high use in MRI. Discussion on a method for reducing current is further examined in sections 6.2.

6.2 Further Improvements

Further improvements upon this control system would include using more advanced hardware for computation and additional circuitry to reduce current used in the magnet room. While all these improvements were considered when building this system, they were unfortunately not implemented due to time constraints and would require the redesign and rebuilding of every element of the entire system from the T/R switches to the phase shifters.

The first improvement is to improve the control system using a Field Programmable Gate Array (FPGA) for faster computation and large memory. Using a device such as an FPGA would the system to take advantage of more complicated hardware than Atmel microcontroller was capable. This gives the system the ability to operating faster and very precise timing on changing the state of the phase shifters. While another device a cheaper device less complicated device such a Programmable Logic Converter (PLC) or a 32-bit microcontroller such as the TI-Delfino could be used, but the throughput would be much lower.

Using the FPGA would allow integrating further with the MRI scanner in order to use the measurement system while the RF pulse is transmitting. Doing so the measurement system could measure the applied phase shift vs required phase shift and change the phase if necessary. This would be done by waking up the microcontroller only while the RF pulse is being applied. This method guarantees that the required phase shift applied is always the applied phase shift and counteract issues from phase inaccuracy of the RF amplifier, phase shifter or coupling on the coil. Unfortunately, this would require a

digitally controllable variable attenuator in order to protect the measurement system when imaging with higher transmit power, but also ensure enough signal is present to make accurate phase measurements.

In order to optimize the dynamic shimming performance of the system requires onboard hardware memory in the form of FIFO (First In First Out) memory could be used. Using hardware designed dedicated memory will remove the Microcontroller and BeagleBone when doing dynamic Shimming and allow the system to be controlled by the scanner [23]. Similar to the current method of dynamic shimming the BeagleBone will spam the microcontroller which will then save data on to a hardware memory queue using a clocking scheme. This method would ideally result in unlimited shim solutions being stored by simply cascading multiple FIFO memory in series Additional glue logic will be required in order to directly attach the trigger line from the scanner directly to the memory so that the host scanner will have complete control of changing between shim solutions. This method has the potential to change between shim solution on the order of a few microseconds.

The most important improvement for this project would be to drive all of the phase shifters and T/R switches in parallel using a driver circuit with an isolated ground. This would basically be accomplished by using the driver circuit to power the control objects, but in order to support multiple devices, this would require that the driver circuit is cascaded till there are enough outputs. Using this method, the amount of generated by a factor of 2^n . Therefore for 3 levels of differential drive circuits would be required for the T/R switches and 4 levels for the phase shifters. The additional circuitry would be placed

right after the current source for the T/R switches this means right after the pin diode driver and for the phase shifter right after the voltage regulator. Using this driver circuit would potentially decrease the current requirements by a factor of two thirds. All eight T/R switches could be driven by using only 400mA and the all 16 phase shifter modules by a factor would only require 3.2A. The difficulty in using the differential drive to power the system is the system would need isolated ground. Currently, the system uses a single ground for Earth, RF, DC, and signal. In order to reduce the current draw, the ground would need to be isolated from other sources. This was primarily not done as it would require that the Phase shifter, T/R switches, and power splitter are rebuilt. The current reeducation primary aid in reducing ground loops which could be created by drawing such a large current on the ground wire. The larger the current the more cause there is for a potential difference to accumulate on the ground. Another issue is safety in MRI it is known that large current near the bore could potentially be dangerous. This is due to the force that is exerted due to a current-carrying wire in a magnetic field. Looking at the equation below the force is directly proportional to current and the magnetic field.

$$F = I\overline{LB}_0 \quad (6.1)$$

6.3 Conclusions

There are many advancements that can still be made to the overall system in order to improve the overall speed and efficacy of the system. Currently, the system is able to meet the overall goal of the project, being able to B₁ Shim given eight B₁ Maps on the 7T

MRI scanner. Testing in the lab using the positioner system and the 7T MRI scanner has shown that the system can move the region of interest imaging inside of the phantom. Furthermore, the system can dynamically switch between shim solutions per RF pulse in less than 10ms. Doing so allows different locations around the phantom to be optimized for multi-slice applications. The ability to dynamically shim to increase the region of interest that is being optimized during imaging entire to optimize the entire phantom at once. Unfortunately, due to limited access to the 7T system, only the static operation has been tested in the lab and at UTSW, but Dynamic operation has only been verified to be functioning within the lab.

REFERENCES

- [1] E. L. Hahn, "Spin echoes," *Physical review*, vol. 80, no. 4, p. 580, 1950.
- [2] E. Fukushima, "Nuclear magnetic resonance as a tool to study flow," *Annual review of fluid mechanics*, vol. 31, no. 1, pp. 95-123, 1999.
- [3] S. Ogawa, T.-M. Lee, A. R. Kay, and D. W. Tank, "Brain magnetic resonance imaging with contrast dependent on blood oxygenation," *proceedings of the National Academy of Sciences*, vol. 87, no. 24, pp. 9868-9872, 1990.
- [4] J. T. Vaughan et al., "7T vs. 4T: RF power, homogeneity, and signal-to-noise comparison in head images," *Magnetic Resonance in Medicine: An Official Journal of the International Society for Magnetic Resonance in Medicine*, vol. 46, no. 1, pp. 24-30, 2001.
- [5] J. T. Vaughan et al., "Whole-body imaging at 7T: preliminary results," *Magnetic Resonance in Medicine: An Official Journal of the International Society for Magnetic Resonance in Medicine*, vol. 61, no. 1, pp. 244-248, 2009.
- [6] G. Adriany et al., "Transmit and receive transmission line arrays for 7 Tesla parallel imaging," *Magnetic Resonance in Medicine: An Official Journal of the International Society for Magnetic Resonance in Medicine*, vol. 53, no. 2, pp. 434-445, 2005.
- [7] A. Fillmer and A. Henning, "Requirements for Optimal B₀ Shimming for a Spectroscopy Voxel in the Frontal Cortex at Ultra-High Fields," in *Proc. Intl. Soc. Mag. Reson. Med*, 1946, vol. 23, p. 2015.

- [8] A. K. Bitz et al., "An 8-channel add-on RF shimming system for whole-body 7 tesla MRI including real-time SAR monitoring," in Proceedings of the 17th Annual Meeting of ISMRM, 2009: Citeseer.
- [9] W. Mao, M. B. Smith, and C. M. Collins, "Exploring the limits of RF shimming for high-field MRI of the human head," *Magnetic Resonance in Medicine: An Official Journal of the International Society for Magnetic Resonance in Medicine*, vol. 56, no. 4, pp. 918-922, 2006.
- [10] O. Kraff, A. Fischer, A. M. Nagel, C. Mönninghoff, and M. E. Ladd, "MRI at 7 Tesla and above: demonstrated and potential capabilities," *Journal of Magnetic Resonance Imaging*, vol. 41, no. 1, pp. 13-33, 2015.
- [11] J. Vaughan et al., "Efficient high-frequency body coil for high-field MRI," *Magnetic Resonance in Medicine: An Official Journal of the International Society for Magnetic Resonance in Medicine*, vol. 52, no. 4, pp. 851-859, 2004.
- [12] P. Yazdanbakhsh et al., "16-bit vector modulator for B1 shimming in 7T MRI," in *Proc. Intl. Soc. Mag. Reson. Med*, 2009, vol. 17, p. 4768.
- [13] G. J. Metzger, C. Snyder, C. Akgun, T. Vaughan, K. Ugurbil, and P. F. Van de Moortele, "Local B1+ shimming for prostate imaging with transceiver arrays at 7T based on subject-dependent transmit phase measurements," *Magnetic Resonance in Medicine: An Official Journal of the International Society for Magnetic Resonance in Medicine*, vol. 59, no. 2, pp. 396-409, 2008.

- [14] X. Yan, Z. Cao, and W. A. Grissom, "Experimental implementation of array-compressed parallel transmission at 7 tesla," *Magnetic resonance in medicine*, vol. 75, no. 6, pp. 2545-2552, 2016.
- [15] V. O. Boer, D. W. Klomp, C. Juchem, P. R. Luijten, and R. A. de Graaf, "Multislice 1H MRSI of the human brain at 7 T using dynamic B0 and B1 shimming," *Magnetic resonance in medicine*, vol. 68, no. 3, pp. 662-670, 2012.
- [16] A. T. Curtis, K. M. Gilbert, L. M. Klassen, J. S. Gati, and R. S. Menon, "Slice-by-slice B1+ shimming at 7 T," *Magnetic resonance in medicine*, vol. 68, no. 4, pp. 1109-1116, 2012.
- [17] E. J. Wilkinson, "An N-way hybrid power divider," *IRE Transactions on microwave theory and techniques*, vol. 8, no. 1, pp. 116-118, 1960.
- [18] B. van den Bergen, C. A. Van den Berg, L. W. Bartels, and J. J. Lagendijk, "7 T body MRI: B1 shimming with simultaneous SAR reduction," *Physics in Medicine & Biology*, vol. 52, no. 17, p. 5429, 2007.
- [19] L. Alon et al., "Transverse slot antennas for high field MRI," *Magnetic resonance in medicine*, vol. 80, no. 3, pp. 1233-1242, 2018.
- [20] L. I. Sacolick, F. Wiesinger, I. Hancu, and M. W. Vogel, "B1 mapping by Bloch-Siegert shift," *Magnetic resonance in medicine*, vol. 63, no. 5, pp. 1315-1322, 2010.
- [21] J. S. Boyer, S. M. Wright, and J. R. Porter, "An automated measurement system for characterization of RF and gradient coil parameters," *Journal of Magnetic Resonance Imaging*, vol. 8, no. 3, pp. 740-747, 1998.

- [22] J. Cui et al., "A switched-mode breast coil for 7 T MRI using forced-current excitation," *IEEE Transactions on Biomedical Engineering*, vol. 62, no. 7, pp. 1777-1783, 2015.
- [23] E. T. Lebsack and S. M. Wright, "Iterative RF pulse refinement for magnetic resonance imaging," *IEEE transactions on biomedical engineering*, vol. 49, no. 1, pp. 41-48, 2002.

APPENDIX A
USER MANUAL AND DEBUG PROCEDURE

A.1 Launching the BeagleBone

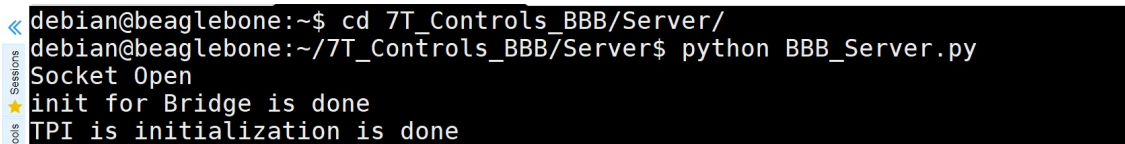
1. The entire must be connected and powered on before the BeagleBone is launched
 - a. BeagleBone must be connected to the TPI
 - b. Fiber Optic cables connected from the BeagleBone to the Controller
 - c. Host Computer(Surface) connected to the mini-USB port of the BeagleBone Box
2. In the event that BeagleBone is set to auto-launch once powered one and after the system is ready this a LED will light up. It will take two minutes.



Figure A-1 – Power supply unit connected for operation

3. If it is desired to run the BeagleBone use Command Lines an SSH Client is necessary such as MobaXterm or Putty will both works, but it is recommended to use MobaXterm

4. Using the SSH Client log into the BeagleBone
 - a. The IP address is “192.168.7.2”
 - b. Username is “debian”
 - c. Password is “temppwd”
5. Next, navigate to the correct directory “cd 7T_Controls_BBB/Server/”
6. Launch the python code using the command “python BBB_Server.py”
 - d. If the program successfully, the window will have some messages(shown below)

A terminal window screenshot showing the execution of a Python script on a BeagleBone. The prompt is 'debian@beaglebone:~\$'. The user enters 'cd 7T_Controls_BBB/Server/'. The prompt changes to 'debian@beaglebone:~/7T_Controls_BBB/Server\$'. The user enters 'python BBB_Server.py'. The output shows 'Socket Open', 'init for Bridge is done', and 'TPI is initialization is done'.

```
<<
debian@beaglebone:~$ cd 7T_Controls_BBB/Server/
debian@beaglebone:~/7T_Controls_BBB/Server$ python BBB_Server.py
Socket Open
init for Bridge is done
TPI is initialization is done
```

Figure A-2 – Terminal output of the BeagleBone being correctly launched

7. Once the Host Computer connects to the BBB additional messages will showing the status of the TPI and MCU.


```
debian@beaglebone:~$ cd 7T_Controls_BBB/Server/
debian@beaglebone:~/7T_Controls_BBB/Server$ python BBB_Server.py
Socket Open
init for Bridge is done
TPI is initialization is done
Received request 'MCU:\xc9'
MCU is doing heartbeat
sent a heartbeat to MCU
Received request 'TPI:WRITE:\xaaU\x00\x02\x08\x01\xf4'
command :
Received request 'TPI:READ:8'
reply :
Received request 'TPI:WRITE:\xaaU\x00\x06\x08\t\xda\x8b\x04\x00\x7f'
command :U
Received request 'TPI:READ:7'
reply :UU
Received request 'TPI:WRITE:\xaaU\x00\x03\x08\n\x00\xea'
command :UU
Received request 'TPI:READ:8'
reply :UU
Received request 'TPI:WRITE:\xaaU\x00\x03\x08\x0b\x01\xe8'
command :UU
Received request 'TPI:READ:7'
reply :UU
Received request 'MCU:\x81'
sent pindiodes to MCU
Received request 'MCU:\x89'
sent pindiodes to MCU
Received request 'MCU:\x91'
sent pindiodes to MCU
Received request 'MCU:\x99'
sent pindiodes to MCU
Received request 'MCU:\xa1'
sent pindiodes to MCU
Received request 'MCU:\xa9'
sent pindiodes to MCU
Received request 'MCU:\xb1'
sent pindiodes to MCU
Received request 'MCU:\xb9'
sent pindiodes to MCU
Received request 'MCU:0'
sent MSBPhaseShiter to MCU
Received request 'MCU:'
```

Figure A-3 – Terminal output of the client computer is correctly connected to the server

8. To change the status of the auto-reboot of the BeagleBone simply use the following lines
 - e. To disable
 - i. `sudo systemctl disable myscrip`
 - f. To enable
 - i. `sudo systemctl enable myscrip`
 - g. Check if the code is running in the background
 - i. `sudo systemctl status myscrip.service`

A.2 Starting the Host Computer

A-2.1 Launching the Host Computer through Executables

1. The default setup on the BeagleBone will launch the code right away so nothing is required here
2. The only thing to do is launch program on the Host Computer. Once BeagleBone is running.
3. Click the Icon “SliceSelectWindow”



Figure A-4 – Desktop executable for the entire system

4. The GUI should automatically Launch if it does not there is an error somewhere
 - a. The most common issue is BeagleBone is not powered on
 - b. For more information reference debug plan
5. If the GUI/code is ever changed then a batch file called “7TBC” has been placed under “7T_Controls_BBB\Client” to generate a new executable

- a. Click once to run, it will take roughly 5 minutes to run
- b. Automatically will update the entire Host computer program the executable will automatically update

A-2.2 Launching the Host Computer through Command line

1. In the event that it is desired to run the from the command line, Windows PowerShell will be the easiest approach
 - a. Use PowerShell navigate to the directory containing the program
 - b. Use this command “cd .\Desktop\7T_Controls_BBB\Client\”
 - c. The path may be different per user or computer
2. Next type in python “python .\SliceSelectWindow.py” and GUI should launch
3. If the program successfully, the GUI will launch, and Power shell will appear to have some messages(shown below)

```
PS C:\Users\Kevinpatel_1996\Desktop\7T_Controls_BBB\Client> python .\SliceSelectWindow.py
Connecting to the server
Socket Open
Setup on Client is done, the MCU has a heartbeat and phase shifters are all set to 0 degrees
TPI is linked
Server is connected
```

Figure A-5 – Terminal output of the client computer being correctly launched

A.3 Functions on the GUI

Function	Description
MCU Control	
Heartbeat	Send a heartbeat function to the MCU to check if the MCU operating correctly
MCU Power	Change that state of the MCU Clock between on and off
Update Phase shifters	Update the state of all 8 of the phase shifters
Take Measurement	Take a measurement for gain & phase and average based on value on in the box above "Number of averages "
Normalize	Normalized all of the phase shifter measurement to Channel 1, will continually update the reference to the phase on Channel 1 per measurement
Calibrate	Normalized all of the phase shifter measurement to Channel 1, will not update the reference to Channel 1 per measurement just once
Test Phase shifters	Flash all of phase shift's controls 5 times
Test System	Launch the Test Window to check if the system is correctly wired and phase shifters are working
Zero Phase	Set all of the phase shifts to 0
In Phase	Find the phase shifts to counteract the phase error per channel
Birdcage Mode	Put the system in phase and then birdcage [0,45,90,....,-45]
Anti-Birdcage Mode	Put the system in phase and then anti birdcage [-45,-90,....,-0]
TPI Control	
Update TPI	Update the TPI's Frequency and output based on the 2 boxes above
TPI power	Update wither the TPI is output or not
Dynamic Shimming	
Generate Table	Generates A table-based of size 8 by x. Where is the number from "Number of slices"
Pulse per slice	Tells the system how Triggers to count before changing to the next shim solution
Start scan	Will tell the system to transfer the phase data over to the MCU and to start waiting for the trigger line
Import Phase data	Import data for all shim solutions from the file "Dynamic Shimming Phases.csv"

Table A-1 – Functions on the GUI

A.4 Setup Procedure for UTSW

1. Equipment room

- a. Power supply unit will be placed under the pentation panel
- b. The power supply unit will be plugged into an isolation transfer which is then connected to any available 120V wall outlet
- c. The power cable will connect to the pentation panel to the through a DE9 connection
- d. Reference signal from amplifier box will connect to the pentation panel through a BNC cable
- e. The 2 PA signal cables will also connect to the pentation panel through a BNC cable and then two 4x1 power splitter within the system rack.
- f. Fiber optic connectors can be feed through the waveguide
- g. Trigger from the RF amplifier's Unblank signal will connect to the Power supply unit's Trigger input and RF amplifiers using a BNC "tee"
- h. Lastly, the Trigger output from the Power supply unit will connect to the Pentation panel for triggering of the T/R switches

2. Magnet room

- a. System rack will be placed to the left of the patient table
- b. Fiber optic connectors and power supply will go directly to the controller in the system rack
- c. TPI ref signal from the amplifier box will connect the signal on the side of the controller

- d. The trigger will connect to the pin diode driver on top of the system rack
 - e. Current probes from dipoles will connect directly to the 8 sma connections on the controller
3. Running the Host Computer
- a. Connect the BeagleBone box to the surface using the Ethernet cable
 - b. Wait for BeagleBone to auto-start to run
 - i. If AutoStart fails, simply login to the BeagleBone and manually launch the code
 - c. Launch the program on the Host computer
 - d. The system should be set up and running at this point with the GUI
4. GUI
- a. Press the “Test Phase Shifters” button
 - i. All phase shifter change colors 10 times
 - b. Press the “Test System” button
 - i. Terminate table should have the red diagonal showing system is hooked up correctly
 - ii. Phase shifter tables should be all 8 channels moving upward linearly

A.5 Setup Procedure for MRSL

Setup of the system for use in the lab at MRSL is very similar to use at UTSW but does not require placing the system around the MRI suite. Testing the system in the lab most likely requires the use of the positioner system in order to generate field maps.

1. The liquid phantom will need to be placed inside of the positioner system.
2. Next, the cross probe will be placed on to platform connected by the stepper motors.
 - a. The cross probe should be placed so that the probe is located near the feed point of the dipoles
3. The VNA will need to be connected in S_{21} mode order to measure gain and phase with the following settings. The TPI will need to be removed and replaced with the transmit signal from the VNA.
 - a. 2 Points per acquisition
 - b. Frequency – 298MHz
 - c. Amplitude – 0dBm
 - d. Resolution bandwidth –1kHz
 - e. Frequency of bandwidth – 0
4. The Body Coil system will need to be connected as it would be in UTSW, but in the lab, it can all placed in the same area
5. The 2 PA in the amplifier box should be directly connected to the System rack
6. A BNC short need to be placed on to the trigger for the pin diode driver of the T/R switches.
7. For testing of the Dynamic Shimming, a Function generator will be needed and connected to the Trigger input
 - a. High Z mode
 - b. 5V – High

- c. 0V – Low
- d. Duty cycle < 50% to resemble an active low signal as the scanner in UTSW would output.

A.6 Debug Procedures

1. Phase measurement system

- a. Make sure that all cables and fibers are correctly connected
- b. Make sure TPI and MCU is turned off during imaging
- c. Make sure that the dipoles are impedance match
 - i. If they are not it will cause an error in the measurement system
 - ii. Typically gain can be measured with some error but not phase will work at all
 - iii. You would expect all the dipoles to have roughly the same gain, but phase has an error or can't be measured at all
- d. If an AD8302 eval-board are damaged
 - i. Replace board with the spare
 - ii. If two are broken, we have the parts to repair it in the lab
- e. Phase measurements are always the same
 - i. Check the switch matrix cables are correctly connected to MCU using a continuity checker using a multimeter
 - ii. Using the TPI to do an S_{21} measurement and make the switch matrix is opening correctly

2. Communication system

- a. Tell the system to measure the phase using 512 averages
 - i. If the led is flashing on the BeagleBone
 - 1. The issue is sending data into the magnet room
 - 2. Try a different BeagleBone
 - ii. If the led is flashing very dim on only the BeagleBone
 - 1. The issue is getting data into the magnet room
 - 2. Replace the BeagleBone
 - 3. Use different Fiber optic cables
 - iii. If we see a led flash on controller and BeagleBone
 - 1. Issue is getting data out of magnet room
 - 2. Verify this by change phases on phase shifters
 - 3. Reprogram the microcontroller or replace it with one that is already programmed

3. Ground Loop

- a. Leave the door open or go into magnet room and see if the Fiber optic lines are blinking
- b. Completely disconnect all equipment that is not essential
 - i. Anything that is connected to the system
 - ii. Or connected to a wall outlet
 - iii. Example
 - 1. Function Generators
 - 2. Oscilloscope

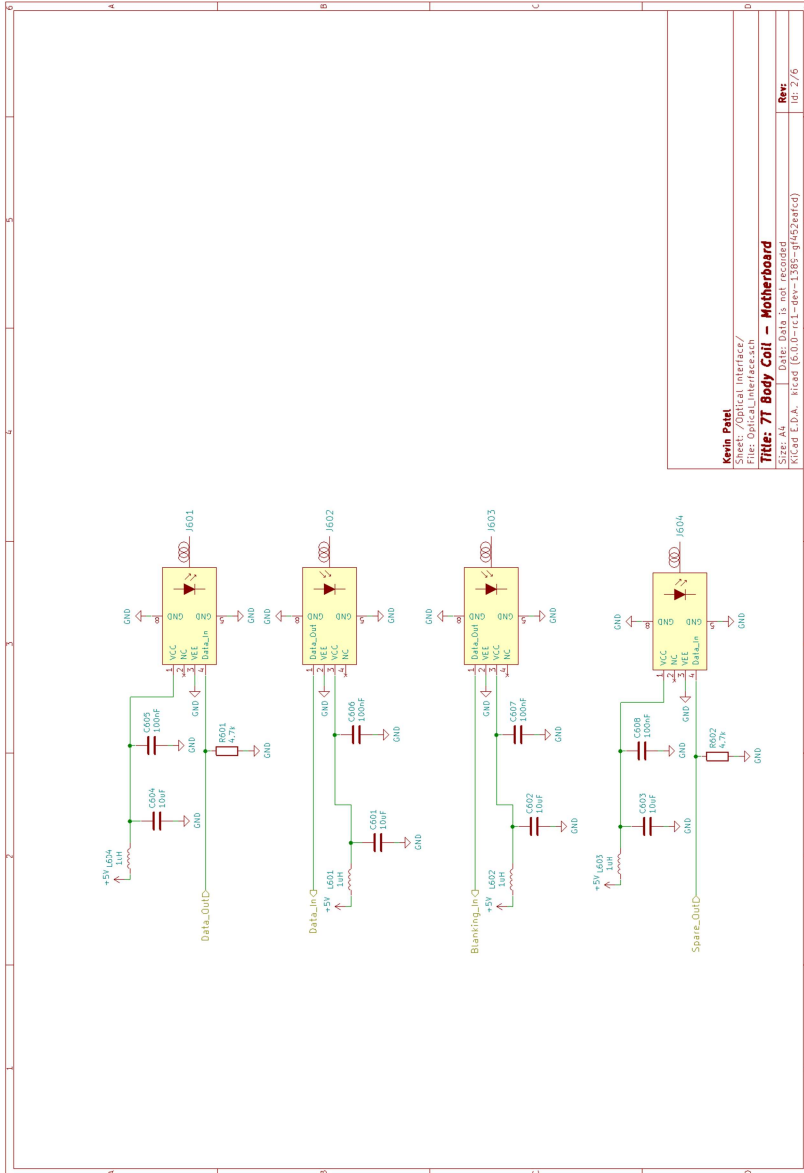
4. Phase shift

- a. Open the controller and see if pin on the MCU has been burned
- b. Open phase shifter and see if anything is damaged
 - i. Replace driver board
 - ii. Toggle phase shifter using a test setup that uses a manual switch to change states
 - iii. Use the Measurement system to make sure that the phase shifters are still working

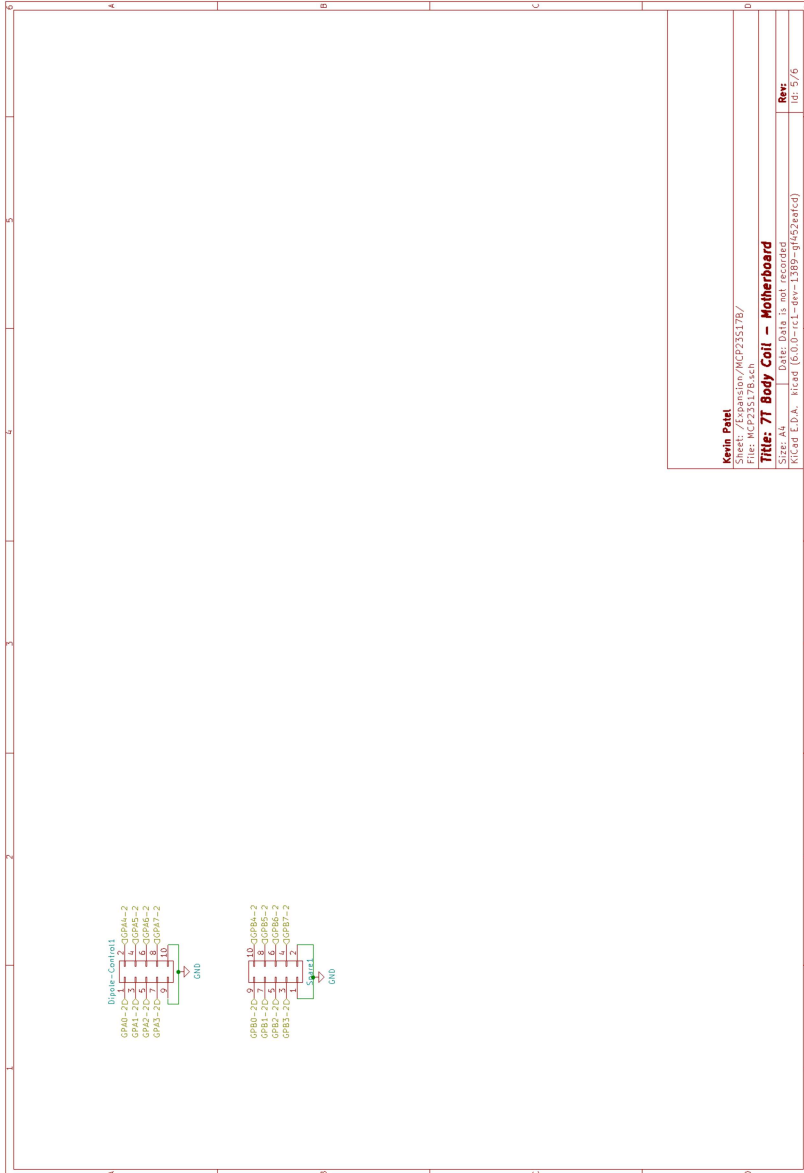
APPENDIX B

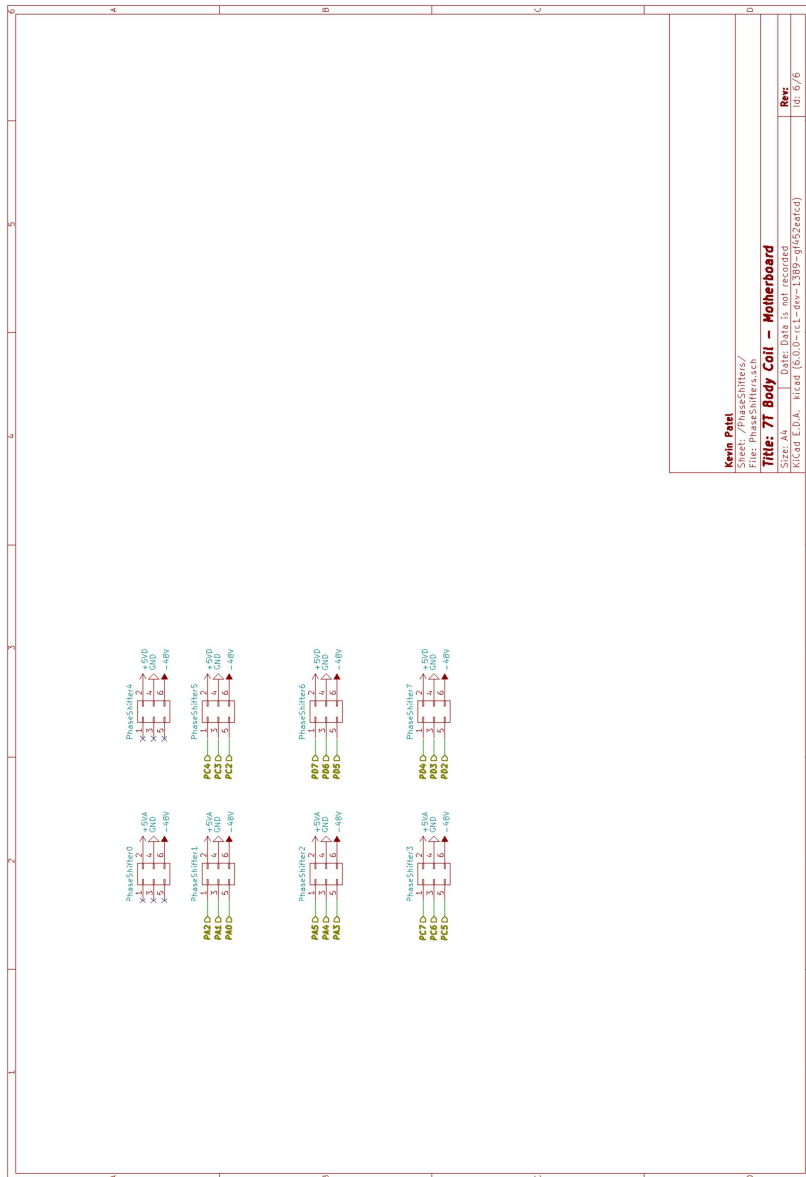
PCBS

This Appendix contains the schematic for all of the major PCBs used in the work done for this thesis.



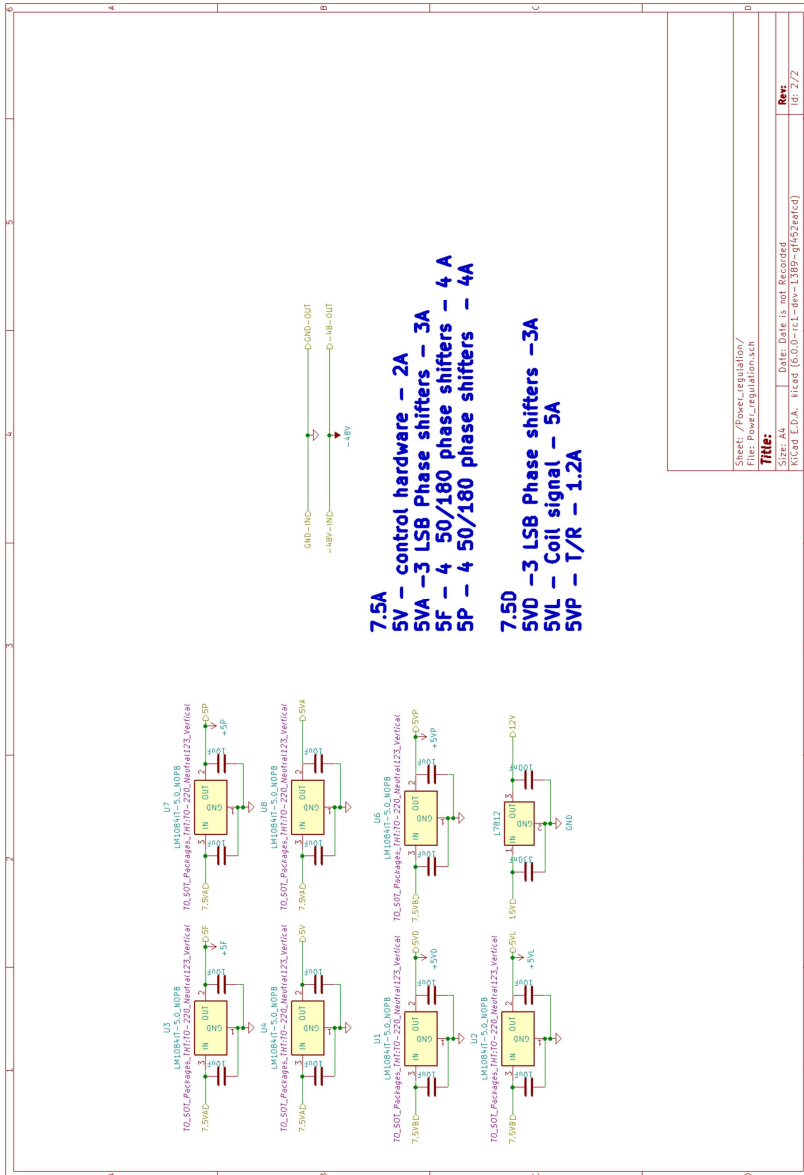
Kevin Patel
 Sheet: /Optical Interface/
 Title: 77 Body Coil - Motherboard
 Rev: 01/2/05
 K:\GD E.D.A. files\600-141-001-1388-01452net(c)





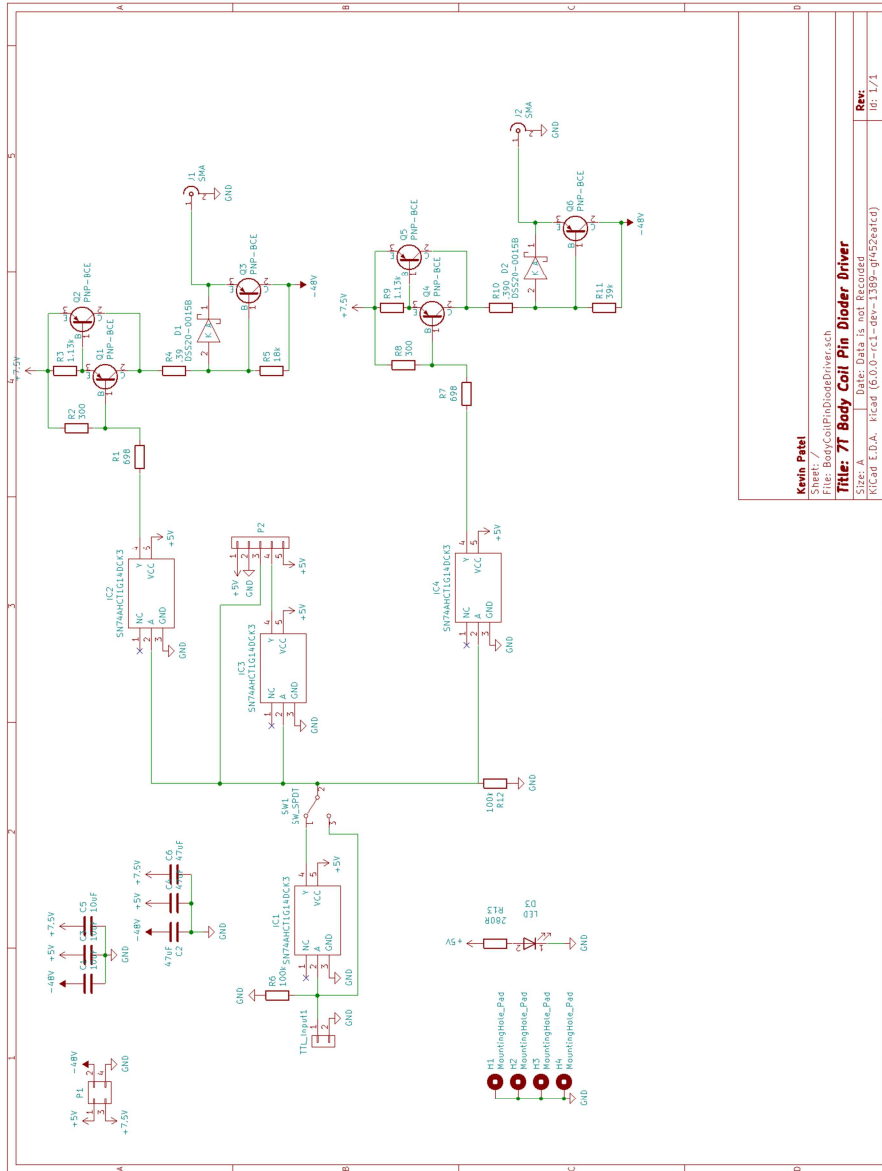
Kevin Patel
 Sheet: /PhaseShifters/
 Project: Motherboard
Title: 77 Body Coil - Motherboard
 Rev: 1
 K:\G01 E.D.A. \Board (6.0.0-rc1-46)-1389-01452\pcb

The motherboard is shown is in Figure 3.11.



The power supply board is shown is in Figure 3.11.

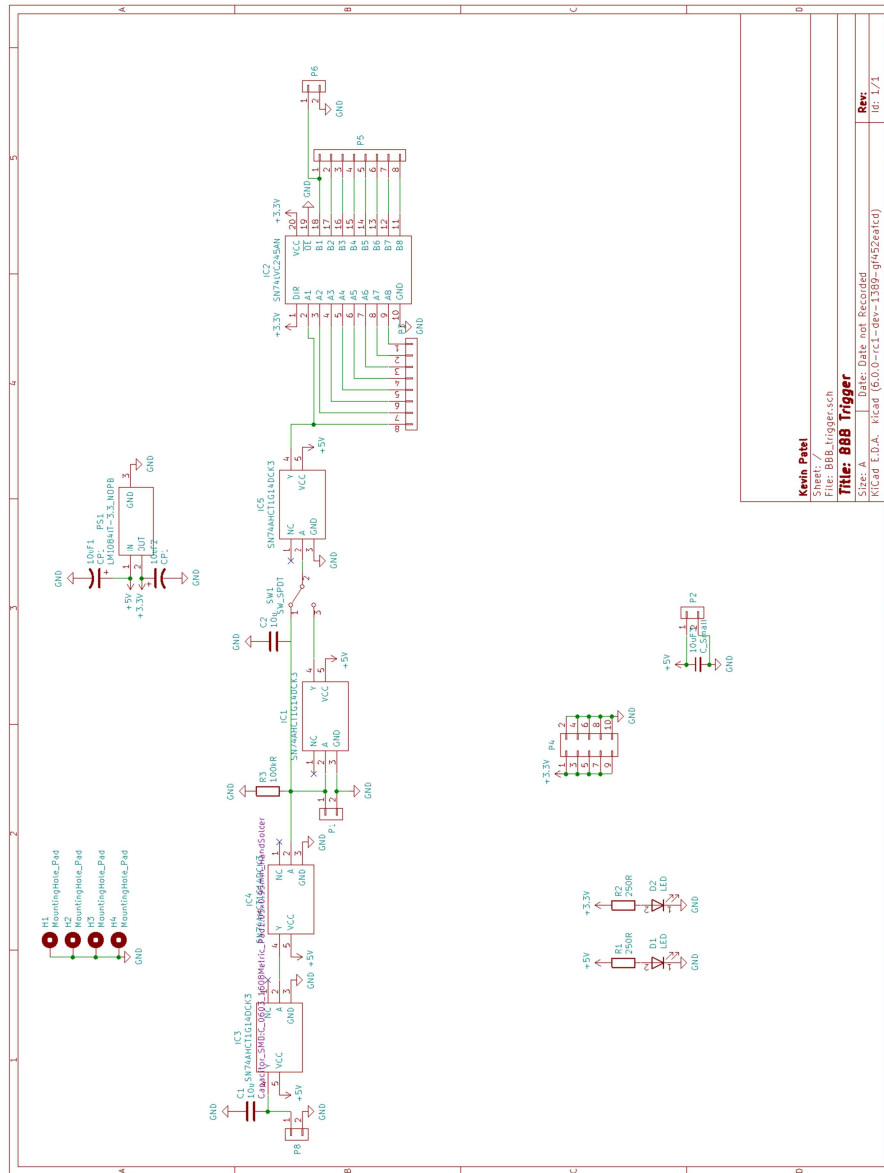
B.3 Pin Diode Driver



Kevin Patel
File: BodyCoilPinDiodeDriver.sch
Title: 7T Body Coil Pin Diode Driver
Sheet: 1
Rev: 1/1

The pin diode driver is shown is in Figure 3.16.

B.4 Trigger Interface for Dynamic Shimming



The trigger interface is shown in Figure 3.8.

APPENDIX C

MATLAB CODE FOR PROCESSING POSITIONER DATA

C.1 Function – pointsToSurf.m

```
function Z = pointsToSurf(x,y,z)
% This function is made to create smooth surfaces from individual scattered
% points

% x, y, z, are the inputs in their respective axes

nx = size(x); ny = size(y); nz = size(z);

cond_vectors = (min(nx)==1 && min(ny)==1 && min(nz)==1);
cond_sizes = (max(nx)==max(ny) && max(ny)==max(nz) && max(nz)==max(nx));

if ~cond_vectors
    disp('All the inputs should be vectors');
end

if ~cond_sizes
    disp('All the inputs should have same maximum size');
end

%% Actual code

% Converting all inputs to uniform column vector
x = x(:); y = y(:); z = z(:);

if cond_vectors && cond_sizes

    n = 200; %n = Number of points desired,
    x_edge=linspace(floor(min(x)),ceil(max(x)),n);
    y_edge=linspace(floor(min(y)),ceil(max(y)),n);

    [X,Y]=meshgrid(x_edge,y_edge);
    Z=griddata(x,y,z,X,Y);
end
```

C.2 Script – Positioner_Plot.m

```
clear all;close all;clc;
%% Read CSV file
data = csvread('053119_highResCenter.csv');
x = data(1:end,1);
y = data(1:end,2);
z = data(1:end,3);
z = 10.^(z/20);
p = data(1:end,4);
%% plot phase
P = pointsToSurf(x,y,p);
P( ~any(P,2), : ) = [];
P = -1*P;
figure(1);imagesc(flip(fliplr(flip(P.'))));colorbar()
%% plot magnitude
Z = pointsToSurf(x,y,z);
Z( ~any(Z,2), : ) = [];
figure(2);imagesc(flip(fliplr(flip(Z.'))));colorbar();
```